GPO PRICE

CSFTI PRICE(S) $ _____

Hard copy (HC) 3.00

FRANKLIN GNO CORPORATION

P O BOX 3250 WEST PALM BEACH FLORIDA 33402

NASA CR-66568

HIGH TEMPERATURE STUDY OF ELECTROPHILIC GASES FOR PLASMA QUENCHING

by

W. D. Kilpatrick

January 18, 1968

Prepared under Contract NAS1-6884 by

Franklin GNO Corporation
West Palm Beach, Florida

for Langley Research Center

NATIONAL AERONAUTICS AND SPACE ADMINISTRATION

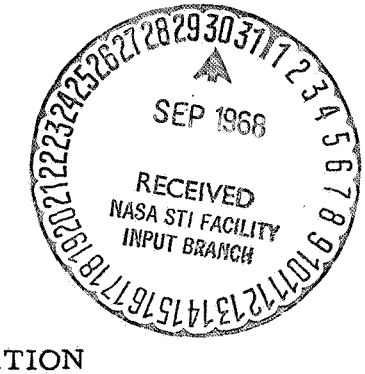

FOREWORD

The object of the following experimental research and measurements program is to obtain electron attachment data for certain gaseous materials. These data find application to the quenching of high temperature plasmas created during atmospheric reentry.

The research was sponsored by the Langley Research Center, National Aeronautics and Space Administration, under Contract NAS1-6884. It covers work completed between January 10, 1967 and January 10, 1968.

Recognition for special contributions to the program are extended to: Mr. Norman Akey; Dr. Martin J. Cohen; for his encouragement during the program; and to Mr. Robert C. Kindel for carrying out most of the details of experimental design and measurement which were encountered.

ABSTRACT

Electron attachment studies were carried out for eight different electrophilic materials through the use of high temperature techniques up to 2000°C. The materials were all liquids with approximate vapor pressure of $0.01 < P < 250$ torr at room temperature, except for SF_6 which was used for reference and calibrations. Not all of the materials were amenable to measurement at 2000°C due to chemical decomposition. The materials examined were C_6F_{14} (perfluorohexane) C_7F_{16} (perfluoroheptane), C_8F_{18} (perfluoroctane), $(C_4F_9)_3$ N (perfluoroamine, also FC-43), Freon E-3, Freon E-5, Freon E-9, and argon which was used as an inert carrier.

Three methods were employed for the various measurements over the temperature range from room temperature to 2000°C: (a) Drift cell for mobility and attachment measurements at room temperature, (b) Static low-pressure oven for breakdown up to 1000°C and (c) Molecular beam for breakdown of mixtures up to 2000°C.

Comparison of the data from the three methods shows that Freon E-9 is highly electrophilic, and retains its electrophilic property under thermal equilibrium to 2000°C. The remaining materials are effective to varying degrees at lower temperatures.

TABLE OF CONTENTS

LIST OF ILLUSTRATIONS

LIST OF TABLES

SECTION I

INTRODUCTION

Reentry communications depend on the penetration of electromagnetic radiation through the flow field which envelops the vehicle. Under certain conditions the flow field contains significant ion and electron densities, enough to cause failure of transmission through the plasma sheath (blackout).

Penetration of electromagnetic radiation through the reentry plasma has wide application to several reentry problems. Motivation for the present studies comes from the NASA Langley Research Center where there are programs dealing with the reentry communications blackout program.

Of several methods available for reduction of the plasma densities, overboard ejection of additives appears both practical and effective. Past efforts in plasma quenching have been partially limited by available materials.

This program describes the results of an experimental research program for determining the effectiveness of several highly stable fluorocarbon compounds as additives for quenching.

Section II covers the background of the communications blackout problem, additives, and the effects to be expected from electron attachment by the fluorocarbon materials. Brief consideration is also given to the general properties of the fluorocarbons, to the formation of their stable negative ions required for electron attachment, and to the measurement of attachment.

The program was divided into three relatively equal parts, each covering a distinct range of experimental temperatures and method of measurement. Section III, IV, and V deal with the different experimental apparatus used, the data acquired by each method of measurement, and the reduction of data. The three efforts were necessary to cover the range of experimental parameters, such as thermal emission, thermal expansion, and chemical interactions with the oven walls. Overlaps in the data from each of the separate methods was expected.

A comparison of the data from all methods is found in Section VI. This section also includes, as far as practicable, a comparison of the present data with other published material in an effort to establish a degree of confidence, with limits, for the present measurements and their application to plasma quenching.

The effect of higher collision frequencies (greater damping) is to reduce the forward and backward re-radiation waves, thus both reflection and transmission attenuation are reduced due to less cancellation with the signal wave.

This simplified picture indicates that reentry attenuation is a problem when transmission frequencies are less than the plasma frequency. Conversely when transmission frequencies exceed the plasma frequency, the electrons appear to have inertia, respond less to the rf fields, and give rise to little attenuation or reflection.

In summary, and from a charged particle point of view, free electrons in the reentry plasma interact with the electric field of the incident rf. Re-radiation from electron motion occurs backward as reflection, and forward as attenuation due to phase cancellation with the incident wave.

An objective of the present program is to alleviate the rf transmission attenuation through the use of suitable materials added to the plasma so that the free electrons are attached to heavy molecules. In this way, the attached electrons are no longer free to interfere with the rf communication transmissions.

2-2. Review of Droplet Ejection

The results of several programs[1-5] at NASA Langley Research Center have shown that the addition of water droplets to a flowing reentry plasma can, under some conditions, cause significant reduction in electron density of the sheath.

As set forth by Evans[4], reduction of the electron density by water droplet ejection is presumed to be due to the large physical cross section of the droplet through which the electron flux in the plasma must pass. Electrons are intercepted by the droplet surface and "captured" until electrostatic repulsion reflects additional electrons away. Further electron acquisition can be made after the addition of positive ions reduces the droplet charge. Thus, given sufficient time, the droplet will assume a surface equilibrium charge much like a conventional plasma probe at floating potential, with equal positive and negative currents to the droplets.

The electrophilic value of water vapor is essentially zero. Therefore, if the liquid surface acts as a catalyst for charge recombination before complete evaporation, there is only a short finite time for attachment. Only if this effective attachment time is longer than physical transport times can transmission through the plasma be considered.

A main concern over the use of water droplet ejection for alleviation of the blackout is the amount of water required to accomplish the job. The use of fluorocarbon additives instead of water appears much more efficient, but judgment as to their effective use must be based on the efficiency of the electron capture mechanisms.

2-3 The Droplet-Vapor System

Water droplet ejection is not clearly the most practical method for plasma quenching. A much more effective plasma quench system can be designed if the vapor, resulting from evaporation of the droplet, were of a high or higher equivalent electrophilic value. One of the critical problems in the design of a droplet-vapor system is the availability of pertinent data for the vapor compounds.

Entirely different mechanisms are involved for electron attachment to liquid droplets, as compared with attachment to molecules in the vapor state. The differences are expressible in terms of electron energy, thermal decomposition, collision frequency and reaction rate. The flow stream concept of reduction in electron population by plasma "cooling" is replaced by a particle concept of attachment by collision, where free electrons in a distribution simply disappear.

Electron attachment to neutral molecules in the vapor state results in the formation of negative ions. Not only must the negative ions be formed, but these negative ions must be stable if blackout is to be avoided. The rate of liquid evaporation can be relatively slow if the full advantage of a droplet-vapor system is to be realized.

2-4 Electron Attachment and Negative Ion Formation

The terminology of negative ions and their formation is so intimately connected with that of electron attachment processes that a definition of terms could be helpful to avoid confusion.

If electron attachment should occur in such a way that the electron could not become free again by some spontaneous process, then a stable negative ion would have been formed,

Generally in the formation of a stable negative ion, a negative ion with finite lifetime is constructed first. But, no matter which occurs, stable negative ions or negative ions with finite lifetime, electron attachment has been involved.

The change from negative ion to stable negative ion is the equivalent of an excited molecular state losing its excess energy by some means and dropping down to a ground state, the state of least energy. In this sense, a stabilizing process is required to reduce the negative ion to a stable negative ion.

Before stabilization, the lifetime for a negative ion is generally short, on the order of microseconds, so that stabilizing processes must occur relatively quickly if one is to make laboratory observations on the stable negative ion. A convenient way (although not the only one) to stabilize the negative ion is to remove molecular vibrational energy by allowing collisions with gas particles. That is, if the gas pressure is high enough, the stabilizing collision may occur within the lifetime of the negative ion, and an observable stable negative ion will result.

Other stabilization means besides gas collisions are:

- Radiation of excess energy
- Dissociation of the negative ion into either unique components or a spectrum of fragment species
- Chemical attachment to another molecular complex
- Electron exchange where the strict concept of stability is extended to include the reaction molecule as well as the original negative ion -- sometimes referred to as rearrangement.

Looking back one step as to why stable negative ions are the exception and not the general case, there are two basic physics conditions which must be satisfied simultaneously when electron attachment occurs -- conservation of energy, and conservation of momentum. In a favorable attachment collision where momentum is conserved, there would most likely be excess energy to form an excited negative ion. The excited negative ion would in turn have a finite lifetime before complete rejection of the excess energy as a detachment.

A resonance capture process can also occur in which the acceptance energy band is so narrow that essentially no excess energy is allowed if attachment is to occur. Because there are so few electrons with the critical energy in a typical spectrum of energies, resonant capture is improbable or conversely takes a long time over many collision trials. But if resonance capture does occur, it could result in a stable negative ion formation.

The halogens form negative ions because they have a large affinity for electrons. That is, once captured it takes a large amount of energy to remove the captured electron. Even so, it is not necessarily easier to form negative halogen ions, compared with other negative ions, because the excess energy of formation must be removed, and has little to do with the electron binding energy.

High molecular weight materials, if they allow electron capture, often exhibit longer lifetimes as negative ions than the simpler negative halogen ions. This is due to the many vibrational and rotational degrees of freedom available in such complex molecules, and allows the excess energy of formation to be distributed over the many degrees of freedom. It would be expected (on the average) therefore, that the excess energy in the excited state could not be reassembled from all the degrees of freedom for precise detachment unless a long time were allowed for the reassemblage.

Details of the structure of the parent molecule are therefore critical insofar as the negative ion properties are concerned. Experimental methods for evaluation of materials are preferred because efforts to compute the negative ion behavior by including the many degrees of freedom is a prodigious task.

2-5 Fluorocarbon Materials

Fluorocarbon compounds have not been found to exist in a natural terrestrial environment, but their structures are analogous to corresponding familiar hydrocarbons. Therefore, the nomenclature here is to prefix the basic hydrocarbon term with "perfluoro" which denotes substitution of fluorine for all hydrogen atoms in the molecule. For example, perfluoroctane is C_8F_{18}, a perfluoroalkane of linear structure.

Physically,[6-7] the saturated fluorocarbons are very insoluble, particularly in water, hydrogen fluoride and alcohols. They are generally poor solvents except for other fluorocarbons or fluorocarbon derivatives. The fluorocarbons which are normally liquid are room temperature, are

generally colorless with melting and boiling points quite close to those of the corresponding hydrocarbons. Surface tensions and refractive indices are very low, lower than those of the organic compounds.

Chemically, the fluorocarbons are essentially inert, and characterized by great thermal stability. Thermal stability is derived from the strong C-F bond ($D(CF_3\text{-}F) = 5.25$ ev* for the bond in carbon tetrafluoride). This energy compares with typical values of 4.4 and 3.6 ev for the ($CH_3\text{-}H$) and ($H_3C\text{-}CH_3$) bonds.**

For the high temperatures encountered in reentry plasmas, it is of major importance to become familiar with the way in which the fluorocarbons decompose. Available data for high temperature chemistry and behavior of the fluorocarbons is very limited at this time. From an experimental hazards point of view, there is much evidence that toxic gases are released, and explosive exothermic reactions can occur at high experimental temperatures. Extreme safety precautions were exercised throughout the program. A brief outline of possible hazards follows before proceeding to the electron attachment measurements.

The high strength bonds of 4-5 ev for the fluorocarbons means that molecular structures should be expected for temperatures in excess of the 2000°C limits of present experiments. And, for the large molecules of interest, it should be anticipated that many molecular fragmentations would occur over the range of experimental temperatures. On the other hand minimum practical temperatures of some fluorocarbon species could be of the order of 400°C. There is also the possibility of chemical reaction with the environment (walls of a vacuum vessel, residual gases, or exhaust fumes), and there may be active byproducts.

Under suitable conditions, reaction with air forms OF_2 and several toxic NF products. These products are soluble in pump oils and thus constitute a continuous hazard even after completion of experiments.

Danger of explosion in experimental apparatus comes from the exothermic release of the high energy of the C-C and C-F bonds. The early history of fluorocarbon syntheses was plagued by the catastrophic loss of apparatus.

*Bonding energy of 1 ev is equivalent to 23.6 K Cal/mole, and D(C-F) represents the dissociation energy of the C-F bond.

**See C. J. Schexnayder, Jr., NASA Technical Note D-1791 (1963)

Most dangerous of the known toxic fluorocarbon derivitives is $(CF_3)_2 C{:}CF_3$ (perfluorobutylene). Whereas toxic threshold limits of 0.1 ppm are advisable for normal fluorocarbon derivitives, there is apparently no present reference or limit for perfluorobutylene because of the high toxicity. Perfluorobutylene apparently disappears above 1000°C, but on the other hand forms again readily when the fluorocarbon gases pass 1000°C going down through a range of temperatures. That is, perfluorobutylene is apparently highly stable below 1000°C!

Breather masks are commonly recommended instead of canister gas masks where there is the possibility of perfluorobutylene or other toxic fluorocarbon derivitive gases. A recommended procedure would include the following:

- Isolation of experimental apparatus from the operator
- Dilution by rapid air changes in the area of the experimental apparatus
- Exhaust all experimental byproducts from high temperature experiments to the outdoors.

The above recommendations represent the combined judgment of several chemists and toxicologists concerned directly with the handling of fluorocarbon materials. All of these recommendations were satisfied in the present experimental program by enclosing all the apparatus in an 8' x 8' x 8' enclosure with air flow exhaust of 2000 cfm. All experimental measurements data were taken from outside the enclosure.

SECTION III

DRIFT CELL MOBILITY MEASUREMENTS AT ROOM TEMPERATURE

Measurements of the attachment coefficient and mobility of negative ions of Freon E-3, Freon E-5, and C_7F_{16} (perfluoroheptane) were made at room temperature in nitrogen. These measurements were made with previously described[8], but slightly modified apparatus. In the following, there is a brief discussion of the apparatus used, modifications and data obtained.

3-1 Description of Method

The drift cell technique permits direct determination of electron attachments per unit length along the direction of applied low electric fields, and of ion mobility of the negative ions formed by electron attachment.

An outline of the apparatus used is shown in Figure 1. Electrons are released from the cathode surface by absorption of ultraviolet radiation from an electrically pulsed light source. The emitted electrons drift from cathode toward collector through the test gas, but under the influence of an applied electric field.

In transit, some of the electrons are captured by collision with electrophilic molecules, while others cross the entire length of the cell without reaction. Electrons arrive rapidly at the collector, and a detailed accounting of their arrival could be used to derive the electron attachment coefficient,but it is convenient to measure the slower negative ions. A grid is used in close proximity to the collector to allow measurement of the charge transport near the collector at the terminous of the drift length.

Sensitivity of the collector circuit is improved through the use of a pre-amplifier and a boxcar integrator[9]. The boxcar integrator is a time-sampling instrument which is sensitive over only a fraction of the drifting ion current time. Results of integrating the time-fraction low signal levels over many pulses is displayed on a chart recorder.

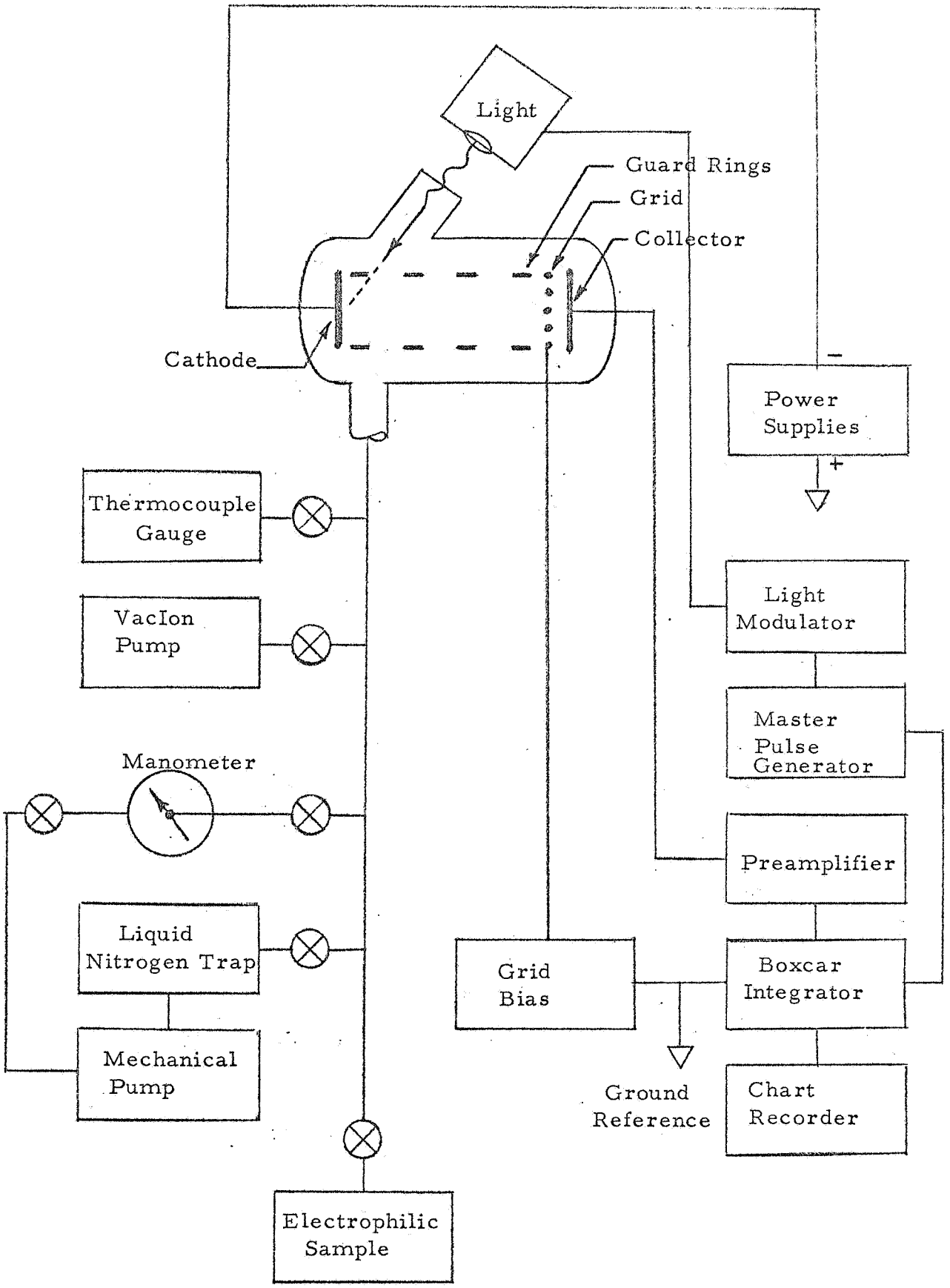

SCHEMATIC DIAGRAM OF DRIFT CHAMBER

FIGURE 1

FRANKLIN GNO CORPORATION

For calculation of the electron attachment, consider an elemental volume

$$dV = dx \cdot dy \cdot dz ,$$

which contains some electrophilic molecules of density n, but mostly neutral molecules of density n_o. If a flux of electrons of average drift velocity v_e passes through dV, the real electron current density j_e will be:

$$j_e = q\, n_e\, v_e, \tag{3-1}$$

where q is the electronic charge, and n_e is the electron density.

The equation of continuity for changes in electron density, including losses by attachment in dV is:

$$dn_e/dt + \nabla \cdot j_e = - \nu_a\, n_e , \tag{3-2}$$

where ν_a is the attachment collision frequency. This becomes

$$(dn_e/dz)\, v_e = - \nu_a\, n_e \tag{3-3}$$

for a steady-state current of one dimension along the direction of the applied field. Solution to this equation is:

$$n_e = n_{e,0} \left[\exp\, (-\nu_a\, z/v_e)\right] , \tag{3-4}$$

where $n_{e,0}$ is the initial electron density at the cathode.

The quantity v_e/ν_a is significant because it represents the average physical distance Δz in the direction of the electric field over which an electron must travel in time $1/\nu_a$ to form a negative ion by molecular attachment. That is, ν_a/v_e is numerically the number of attachments per unit length experienced per molecule along the applied fields direction. That is,

$$\eta = \nu_a / v_e \cdot \tag{3-5}$$

Assuming that the ratio of drift velocities v_e to thermal velocity v is very small, then η would be isotropic and independent of electric field effects. The ratio η/P^* is proportional to the electron attachment cross-section.

*The pressure P is the electrophilic pressure. In cases of gas mixtures, P designates the electrophilic pressure as a component of the total gas pressure P_T.

Primarily ion currents and not electron currents are considered. The changes in negative ion currents show the changes in concentration dn_i/dt, so that

$$dn_i/dt = -dn_e/dt. \tag{3-6}$$

Therefore, steady state ion currents would be

$$n_i = n_{e,0} \left[\exp(-\eta z)\right]. \tag{3-7}$$

For pulsed operation, where it is desired to distinguish electrons from negative ions by their differences in mobility, short light pulses are used. These short pulses also allow only small displacements of either molecules or negative ions during the period when the electron current is available for electron attachment. Therefore, the negative ion current, i, in the vicinity of the grid-collector region would be

$$i = i_o \ (\eta v_i t), \tag{3-8}$$

where i_o is the initial current reaching the collector, v_i is the ion drift velocity down the field and t is the time for a negative ion to move from the point of electron attachment to the collector.

A value for ηv_i is determined from the slope of a plot of log $i \sim t$. v_i is derived from the time required for an ion to traverse the entire length between cathode and grid.

3-2 Drift Cell Experimental Data

Prior data using the drift cell technique for fluorocarbons[8] were obtained with air as background gas, whereas the present data employs pure nitrogen. The reason for the change is to avoid confusion between the formation of negative oxygen ions and negative fluorocarbon ions at small sample concentrations. Mobility data is not greatly affected.

Although oxygen has a very small probability for negative ion formation, large amounts of oxygen in air compete for electron attachment against the high attachment probability of small fluorocarbon concentrations -- the important quantity involved is the product $n\sigma$ (gas density x attachment cross-section).

The drift cell apparatus was modified to measure more than negative ion mobilities. An equilibrium electron distribution is established while electric fields are present during the light pulse. This arrangement allows determination of electron attachment through the use of curves of log i ~ t for each negative ion species.

Figure 2 shows the drift cell dimensions and typical operating potentials. Background pressures in the apparatus before measurements were of the order of 10^{-6} torr, although the heating of the oven was more important for decontamination than background pump-out.

3-2-1 Freon E-3 with Nitrogen in the Drift Cell

It was assumed that Freon E-3 negative ions are formed by capture of free electrons, vibrational excitation of the molecular ion occurs, and stabilization follows from a subsequent gas collision. Accordingly only one negative ion species would be expected, in agreement with experimental observation.

Thus, background gas pressure and electron energy are important in determining the formation of observable negative ions of Freon E-3.

It was possible to change the pressure of Freon E-3 in the drift tube experiments, to change the nitrogen background gas pressure, and to change the applied electric fields. With these experimental parameters short negative ion lifetimes should be detectable. That is, if a pressure effect were observed in the drift cell data for Freon E-3, it would indicate short negative ion lifetimes. The effect would be obtained from a series of values for E/P, or E/P_T, and the data would show pressure as a parameter.

Figure 3 shows several curves of negative ion currents vs delay time under various conditions. For each curve, the photo electron current duration was about 1 millisecond. Electron currents were omitted for convenience. The transit time of the negative ion peak gives a measure of the drift velocity and is used for calculating ion mobilities. The rising slope of the ion current is used to determine the attachment coefficient (a greater slope means a greater attachment coefficient).

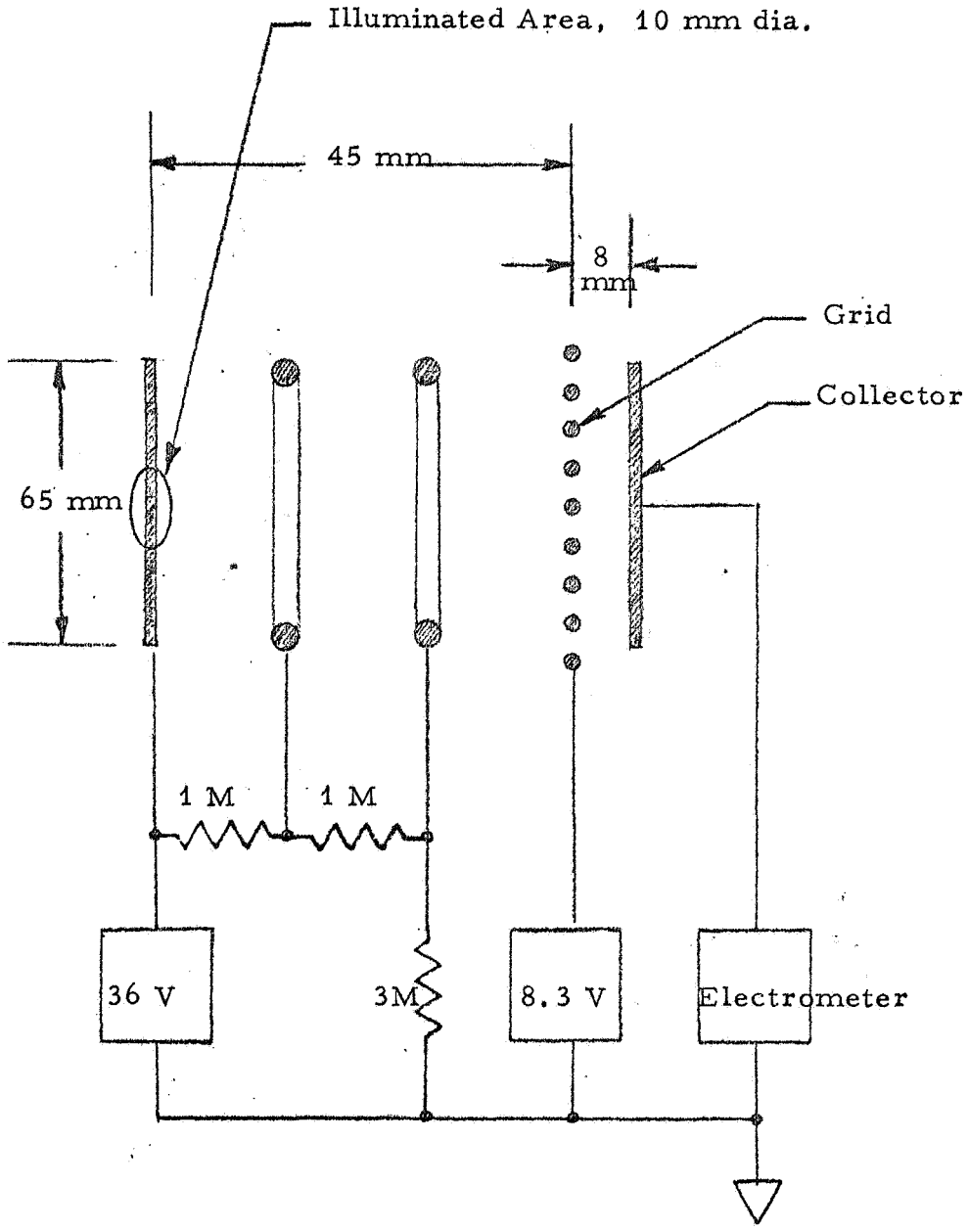

DRIFT CELL DIMENSIONS AND TYPICAL OPERATING POTENTIALS

FIGURE 2

FRANKLIN GNO CORPORATION

These data in Figure 3 were taken at different cell voltages, nitrogen pressures, and pressures of Freon E-3 to ascertain the effect of pressure (if any) on the probability of electron capture and negative ion formation. No pressure effects were observed.

During the course of the measurements, it became clear that the greatest errors were traceable to pressure measurement techniques, and long times were required to establish pressure equilibrium. The important and difficult part was to determine the fraction of Freon E-3 present during the actual measurements.

3-2-2 Freon E-5 and C_7F_{16} with Nitrogen in the Drift Cell

Data from Freon E-5 and C_7F_{16} were taken similar to that for Freon E-3 except that the lower room temperature pressures of Freon E-5 limited the range of the experimental variables. On the other hand, the vapor pressures for C_7F_{16} are much greater than needed for fractional mixtures in nitrogen, so that errors in pressure determination are correspondingly reduced.

Figure 4 shows negative ion current versus time for Freon E-5 in nitrogen. In most respects, the curve is very much like that for Freon E-3 in nitrogen.

Figure 5 shows results for C_7F_{16} in nitrogen. The appearance of multiple components complicates interpretation. The presence of these components from C_7F_{16} could have come about in several ways, but the overall effect is dissimilar to that found in forming O^- from O_2. This is because two species (peaks of the curve) are formed concurrently. Experimentally, changes in both background pressure and electric fields are required for separating the background pressure effect. It was desirable to obtain additional data for different pressures with C_7F_{16} but these data could not be obtained at the time of measurement.

Figure 6 shows the fluorocarbon vapor pressures used for the fluorocarbon experiments.

3-3 Drift Cell Data Summary

Both mobility and attachment coefficients have been determined from the experimental data. Tables I, II, and III show the results of calculations as well as the experimental conditions associated with them.

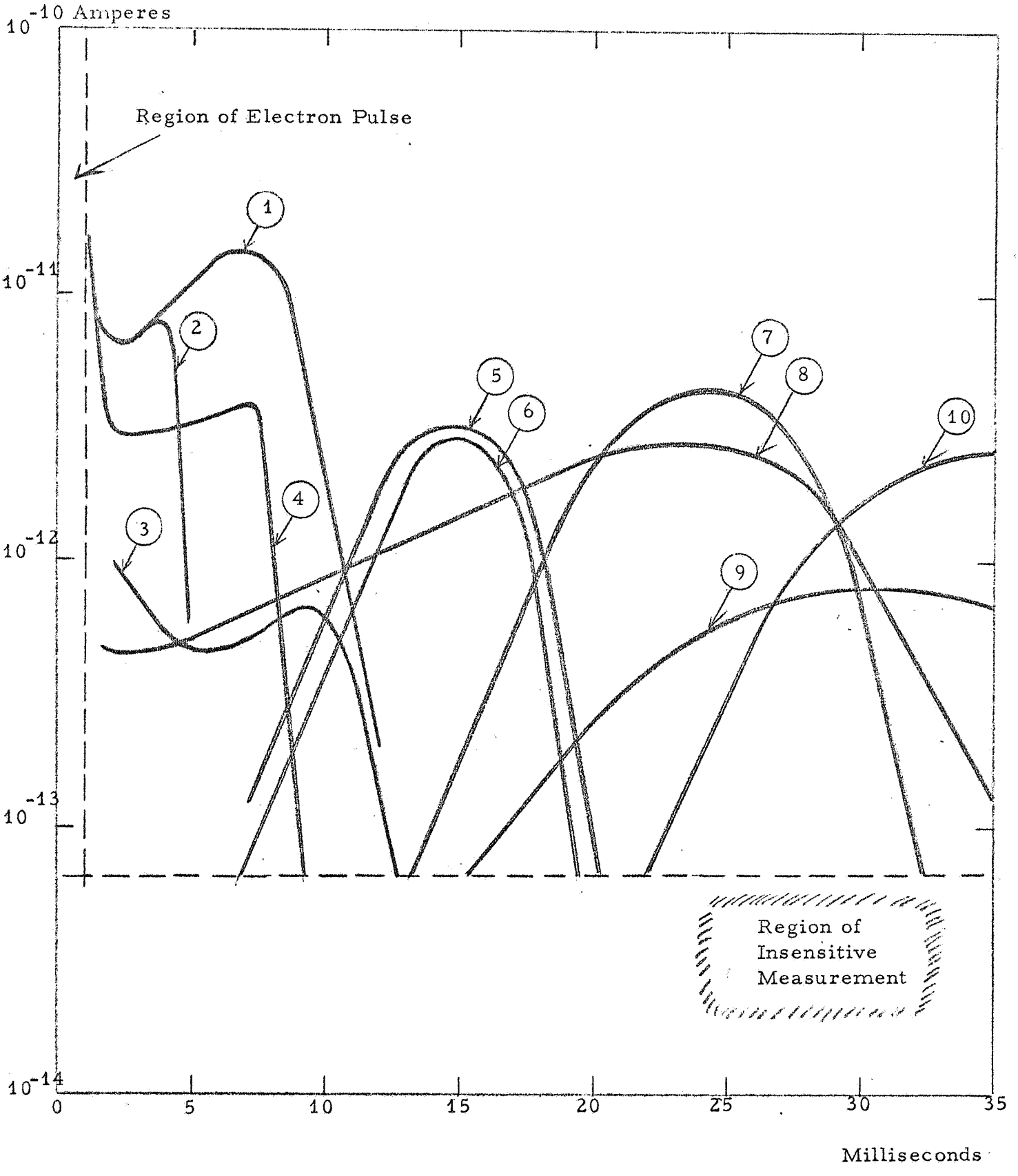

NEGATIVE ION CURRENTS OF FREON E-3

IN NITROGEN, See Table I for Conditions

FRANKLIN GNO CORPORATION

FIGURE 3

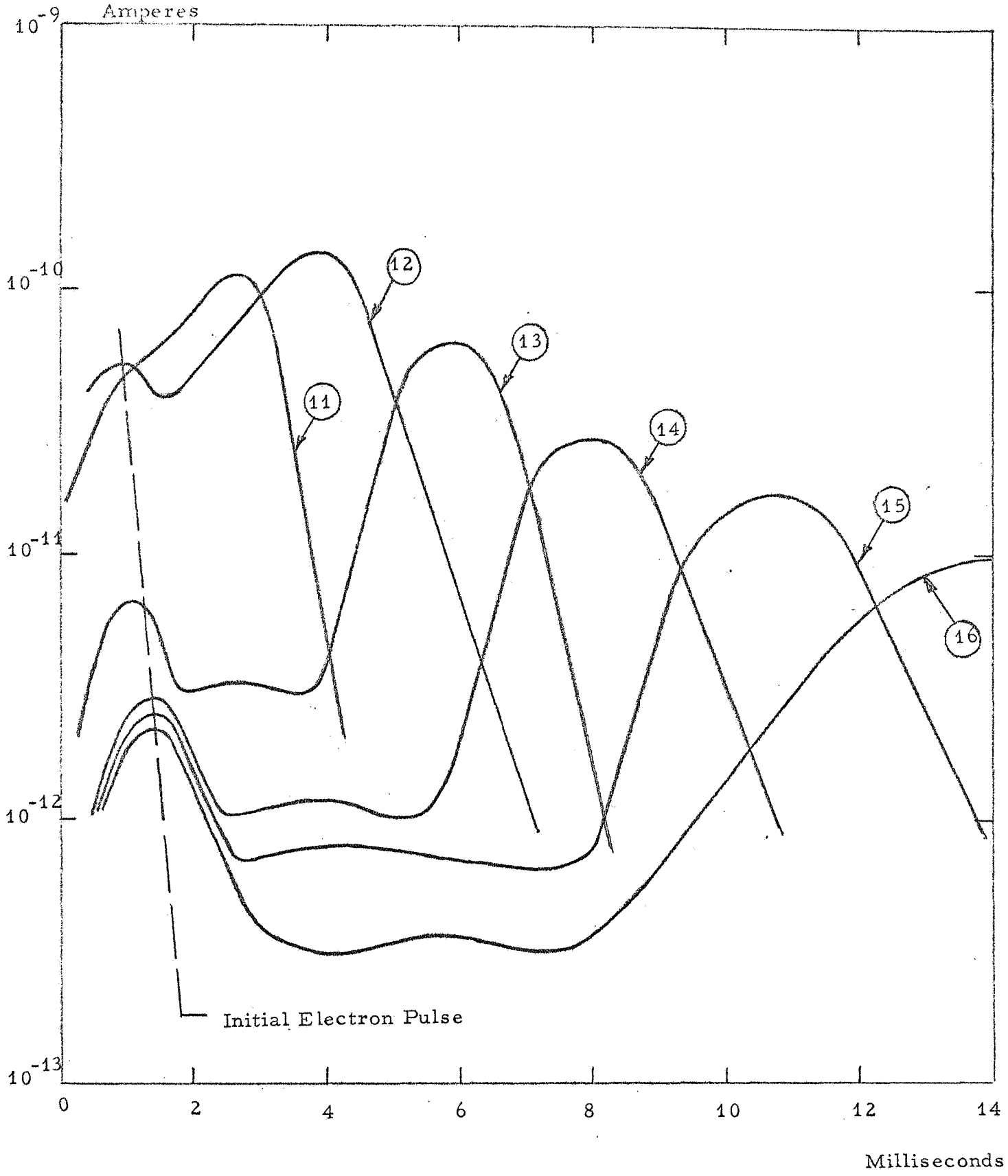

NEGATIVE ION CURRENTS OF FREON E-5

IN NITROGEN (See Table II for Conditions)

FRANKLIN GNO CORPORATION

FIGURE 4

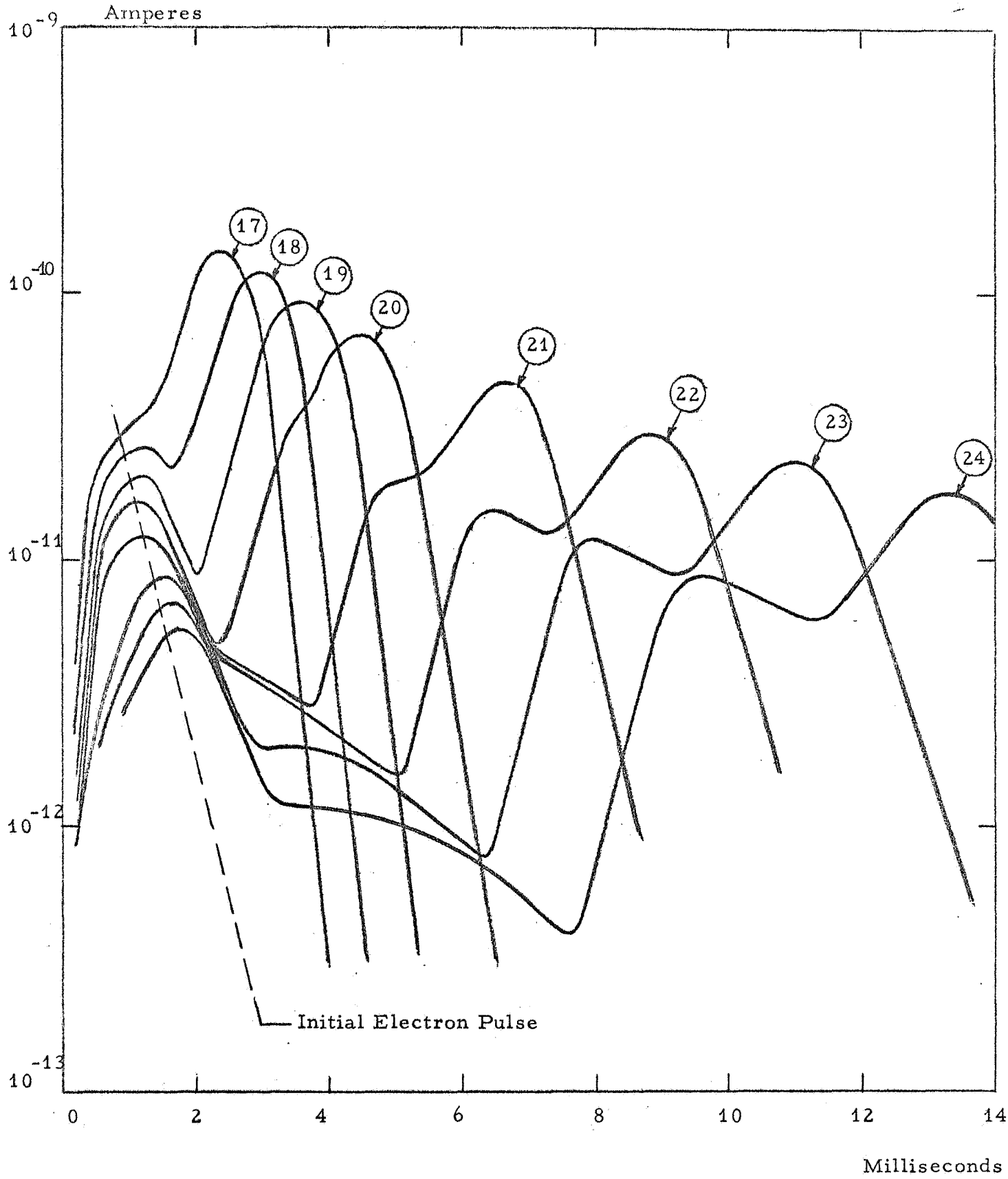

NEGATIVE ION CURRENTS OF C_7F_{16}

IN NITROGEN (See Table III for conditions)

FRANKLIN GNO CORPORATION

FIGURE 5

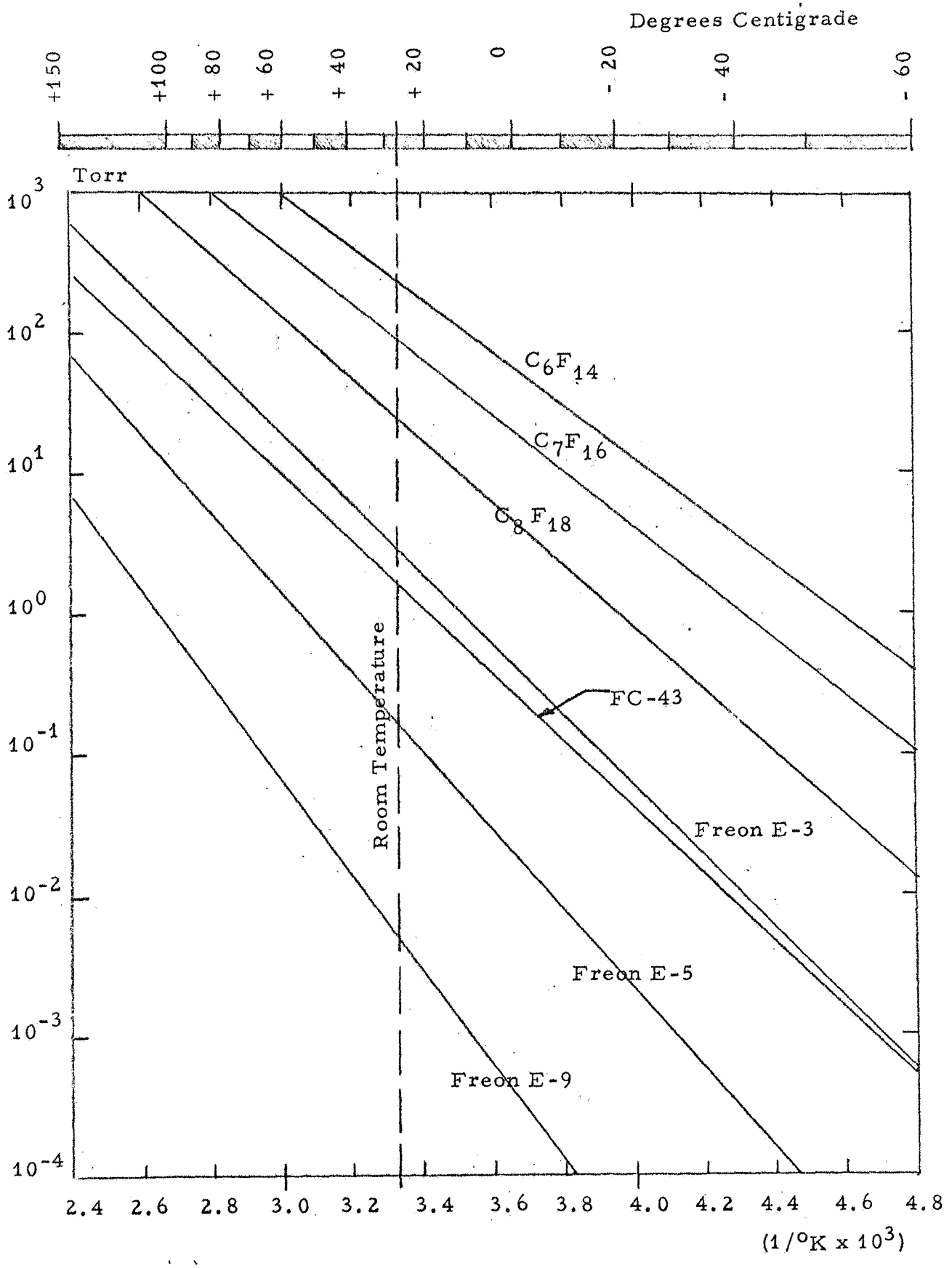

VAPOR PRESSURES USED FOR FLUOROCARBONS IN THIS REPORT

FIGURE 6

FRANKLIN GNO CORPORATION

TABLE I

DRIFT CELL DATA SHEET FOR FREON E-3 IN NITROGEN

(Ref. Figure 3)

Curve (Fig. 3)	Run (Lab)	V (volts)	P_T (torr)	P_3 (torr)	Drift Time (ms)	P_3/P_T	E/P_T	μ_o	η/P_3
1	62	30.0	0.44	0.44	6.9	1.00	14.5	0.06	0.69
2	33	30.0	1.0	0.51	2.9	0.51	6.7	0.31	1.35
3	72	4.3	1.3	0.09	9.6	0.07	0.7	0.84	--
4	36	30.0	2.5	0.51	6.4	0.20	2.7	0.35	1.6
5	56	21.5	2.6	2.6	15.7	1.00	1.8	0.20	0.67
6	31	30.0	2.5	1.2	15.5	0.48	2.7	0.14	0.19
7	58	21.5	5.0	0.5	23.	0.10	0.96	0.27	0.9
8	63	21.5	10.0	0.46	24.	0.05	0.47	0.52	1.1
9	75	4.3	0.5	0.46	28.	1.00	2.1	0.10	0.78
10	59	21.5	10.0	0.5	35.	0.05	0.5	0.37	2.7
--	52	21.5	2.5	0.04	4.7	0.016	1.9	0.66	1.1
--	54	21.5	10	0.04	17.	0.004	0.48	0.73	0.30
--	57	21.5	2.6	2.6	15.	1.00	1.8	0.20	2.9
--	80	4.3	0.13	0.13	8.2	1.00	7.4	--	--
--	Ka	190.	50.8	--	19.	--	0.83	0.38	--

Notes:

- Drift length = 4.5 cm (see Figure 2)
- Voltages V are between grid and cathode
- P_3 represents the partial vapor pressure of Freon E-3, and P_T is the total pressure in the drift cell. For this table $P = P_3$.
- η is the attachment coefficient, the number of electron attachments per unit length along the electric field for pressure P_T.
- μ_o is the negative ion observed mobility, but "reduced to 760 torr".

TABLE II

DRIFT CELL DATA SHEET FOR FREON E-5 IN NITROGEN (Ref. Figure 4)

Curve (Fig.4)	Run (Lab)	V (volts)	P_T (torr)	P_5 (torr)	Drift Time (ms)	P_5/P_T	E/P_T	μ_o	η/P_5
11	83	21.5	1.0	0.11	2.45	0.11	4.8	0.51	14.2
12	84	21.5	2.5	0.11	4.7	0.04	1.9	0.66	9.6
13	97	143	14.0	0.11	6.45	0.008	2.3	0.40	32.
14	103	143	25.4	0.11	9.1	0.0043	1.2	0.52	30.
15	104	143	38.0	0.11	12.0	0.0029	0.83	0.60	34.
16	105	143	50.4	0.11	15.7	0.0022	0.63	0.60	22.

Notes:

- P_5 refers to the partial pressure of Freon E-5. For this table $P = P_5$
- Drift length = 4.5 cm (see Figure 2)
- P_T is total pressure in the cell.

TABLE III

DRIFT CELL DATA FOR C_7F_{16} IN NITROGEN

(Ref. Figure 5)

Curve (Fig. 5)	Run (Lab)	V (volts)	P_T (torr)	P_7 (torr)	Drift Time (ms)	P_7/P_T	E/P_T	μ_o	η/P_7
17	134	154	2.5	.35	2.0	.14	13.7	.29	4.4
18	137	154	6.3	.35	3.5	.056	5.4	.31	4.3
19	138	154	8.9	.35	4.2	.039	3.8	.38	4.4
20	139	154	14.0	.35	5.1	.025	2.4	.47	--
21	141	154	25.4	.35	7.3	.014	1.35	.63	4.9
22	142	154	38.1	.35	9.6	.0092	0.90	.69	6.3
23	143	154	50.8	.35	11.8	.0069	0.67	.75	6.6
24	144	154	63.5	.35	14.5	.0055	0.54	.75	6.5

Notes:

- All values of η/P_7 and μ_o are for second peak (greatest mobility)
- Drift length = 4.5 cm (see Figure 2)
- P_7 refers to the partial pressure of C_7F_{16}, and for this table $P = P_7$.

These results are further summarized in Figure 7 and Table IV. The curves show the η/P, the attachment coefficient per pressure, drawn against the electric field per unit pressure. These curves represent the shape of electron attachment cross section as a function of incident electron energy (proportional to E/P_T).

Four reference curves have been included in Figure 7. The limited curve of values for SF_6 was obtained from the work of Reeves and Geballe[11]. Reference for O^- is derived partly from the data of Phelps, Biondi and Chanin[10], and partly from that of Reeves and Geballe[11]. The curve for O_2^- is for 50 torr (Reference 10).

Most experimental points were obtained for Freon E-3, and there is a large spread in these points. The reason for the spread is not clear at this time, but there is no observable systematic variation with electrophilic pressure or total pressure, in contrast to the data for O_2^- (Reference 9). The greatest experimental errors come from the partial pressure determination of Freon E-3.

Perfluoroheptane (C_7F_{16}) behavior was quite different from Freon E-3. The most significant observation is that a "jump" in η/P occurs at E/P_T about 1 volt/torr .cm (the order of 1 electron volt in electron energy). Reference to Figure 5 will clarify the reason for appearance of the "jump" in the calculation, but will not explain its presence. Two distinct "peaks" appear in the drift cell current. At low pressures, (curves 17, 18, 19) the slope di/dt of the trace is primarily composed of the early peak, say peak No. 1. Because the slope is used to derive the attachment coefficient, the attachment coefficient is essentially that for peak No. 1. Further along in time, peak No. 2 has a measurable slope, and this slope gives rise to the higher attachment coefficient at lower values of E/P_T. In effect, the drift cell method apparently allows for attachment by two different species!

Freon E-5 data has fewer data points, but these data were easily reproducible and were systematic as shown in Figure 4. The apparent attachment of Freon E-5 is greater than that of SF_6 by at least an order of magnitude, and greater than O_2^- by two orders for $1 < E/P_T < 10$. The vapor pressure of Freon E-5 is low, about 0.15 torr at room temperature so that higher partial pressures could not be obtained unless the entire apparatus were heated to prevent condensation.

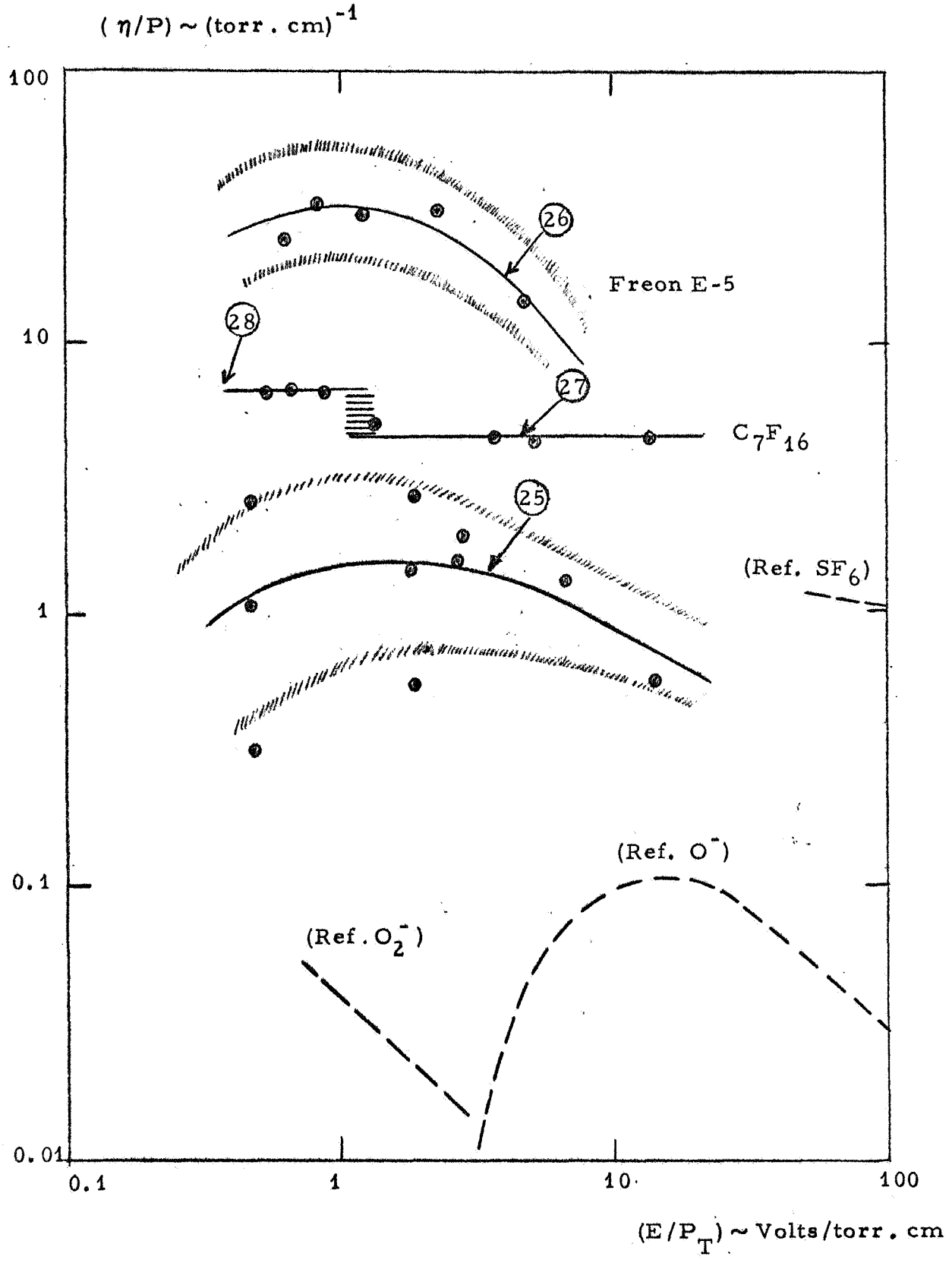

DRIFT CELL ATTACHMENT AS A FUNCTION OF E/P_T IN NITROGEN

FIGURE 7

FRANKLIN GNO CORPORATION

In summary, and in order, values for electron attachment, $\eta/P \approx 1$ are: $4.5 \pm .06$ for C_7F_{16}, 2.5 ± 0.9 for Freon E-3, and 25 ± 5 for Freon 3-5. Values for the mobility of these materials is much lower than expected from conventional theory, and the reason for this is not apparent. All drift cell results were obtained with room temperature apparatus.

SECTION IV

STATIC GAS PRESSURE OVEN BREAKDOWN MEASUREMENT TO 1000°C

Of many molecular species which are capable of attaching free electrons, applicability to reentry depends to a great extent on chemical stability at high temperatures. High molecular weight gases are preferable because the many degrees of freedom of the molecule configuration contribute to long negative ion lifetimes, but on the other hand the larger molecules tend toward weaker bonds and fragment at lower temperatures.

Consequently, previous attachment measurements were extended to high temperatures. A satisfactory combination of both thermal stability and electron attachment is required for reentry application.

Ideally, if data similar to that for the room temperature drift cell could be obtained with a thermally heated cell, it would be satisfactory. There are several reasons why the method cannot be extended to high temperatures. Therefore, an alternate method was devised whereby the influence of high temperatures on the fluorocarbons was conducted with high voltage breakdown techniques.

4-1 Background for Breakdown Measurements

Upon heating a drift cell, electron emission will eventually occur from the walls of the vessel and the electrode structures, and pulsed electron currents required for time-of-flight measurements cannot be distinguished from background currents.

For the higher temperatures, it would be desirable to exclude wall effects entirely from the electron attachment measurement if possible. To do this, the breakdown measurement efforts were divided into two parts. Firstly, a two electrode breakdown cell was made to accommodate static gas breakdown measurements. Secondly, a heated molecular gas stream was directed to flow between cold test electrodes, thus removing electron emission from initiation of the breakdown.

In both cases, thermal equilibrium was established with surface walls in an oven before electron attachment measurements were made. Values of E/P for electrical breakdown are higher than for the drift cell method, but the data are useful to allow evaluation of the electrophilic materials at high temperatures. Mobility data from the breakdown method cannot be obtained unless a time-of-flight determination is included by quenching of the breakdown avalanche. No high temperature mobility data however were taken.

4-1-1 Outline of the Breakdown Method

An abrupt change in electrical resistance between electrodes, as the voltage between them is increased, constitutes a high voltage breakdown. With gas between the electrodes (therefore a gas breakdown), the phenomenon generally depends more on gas characteristics than on electrode surface conditions.

The relationship governing gas breakdown is derived from an expression for pre-breakdown current amplification.

$$i/i_o = \frac{\left[\alpha/(\alpha-\eta)\right]\left[\exp(\alpha-n)\,\delta\right] - \eta/(\alpha-\eta)}{1 - \left[\gamma\,\alpha/(\alpha-\eta)\right]\left[\exp(\alpha-\eta)\,\delta - 1\right]} \tag{4-1}$$

Here, the current i is initially i_o, δ is the electrode separation, γ is the secondary electron coefficient of the electrode surface, and α and η are the ionization and attachment coefficient respectively. When $(i/i_o) \rightarrow \infty$ for breakdown, the denominator vanishes, giving the breakdown criteria,

$$\exp(\alpha - \eta)\,\delta = 1 + (\alpha - \eta)/\gamma\,\alpha \tag{4-2}$$

A simple physical interpretation of this breakdown condition requires that changes in η are measured by changes in α, $d\alpha = d\eta$ near the breakdown region.

Accordingly argon was chosen as an inert gas, small traces of the electrophilic gas were added, and changes in breakdown were measured.

Figure 8 shows the variation of the argon ionization coefficient as a function of E/P over the range of interest to the experiments for fluorocarbon traces. Changes in the experimentally observed breakdown values of E/P appear as a corresponding change of amount $\Delta\alpha$ in α. The change is interpretable directly as the value of η.

4-1-2 Apparatus for Static Breakdown Oven Tests

Figure 9 shows the arrangement for conducting static breakdown experiments up to 1000°C.

The vacuum vessel consists of a glass cross of 6 inches nominal diameter fitted with flat lucite flange plates. The insulating lucite flanges form an ideal construction base for electrical input leads to the test oven.

Under normal operation and after heating for removal of background gases, the vacuum valve is shut to allow for an equilibrium pressure of the electrophilic test gas in the vacuum vessel. An uncontaminated source of test gas is assured in the breakdown region between electrodes if the vacuum valve is "cracked open" slightly to purge the test region continually after the breakdown events. Nominally a breakdown rate of 1 per minute, and a bleedoff of about 1 percent of the equilibrium pressure admits immeasurable variation.

The electrodes are made of molybdenum and the shape of the electrode structure fits a concentric support structure. In this way, the oven shielding is an "integral part" of the electrode structure, and only one high voltage feed through is required for the other active electrode.

4-2 Data for Static 1000°C Breakdown Oven

Calibration of the system was accomplished with the use of SF_6. An accurate linear expansion for breakdown was used[8],

$$V_s = k_1 P\delta + k_2 , \tag{4-3}$$

where V_s is the breakdown across a gap δ with gas pressure, P, and k_1 and k_2 are constants (k_1 = 117 and k_2 = 600 for SF_6). Using these constants, δ = 0.157 cm when pure SF_6 was used in the gap.

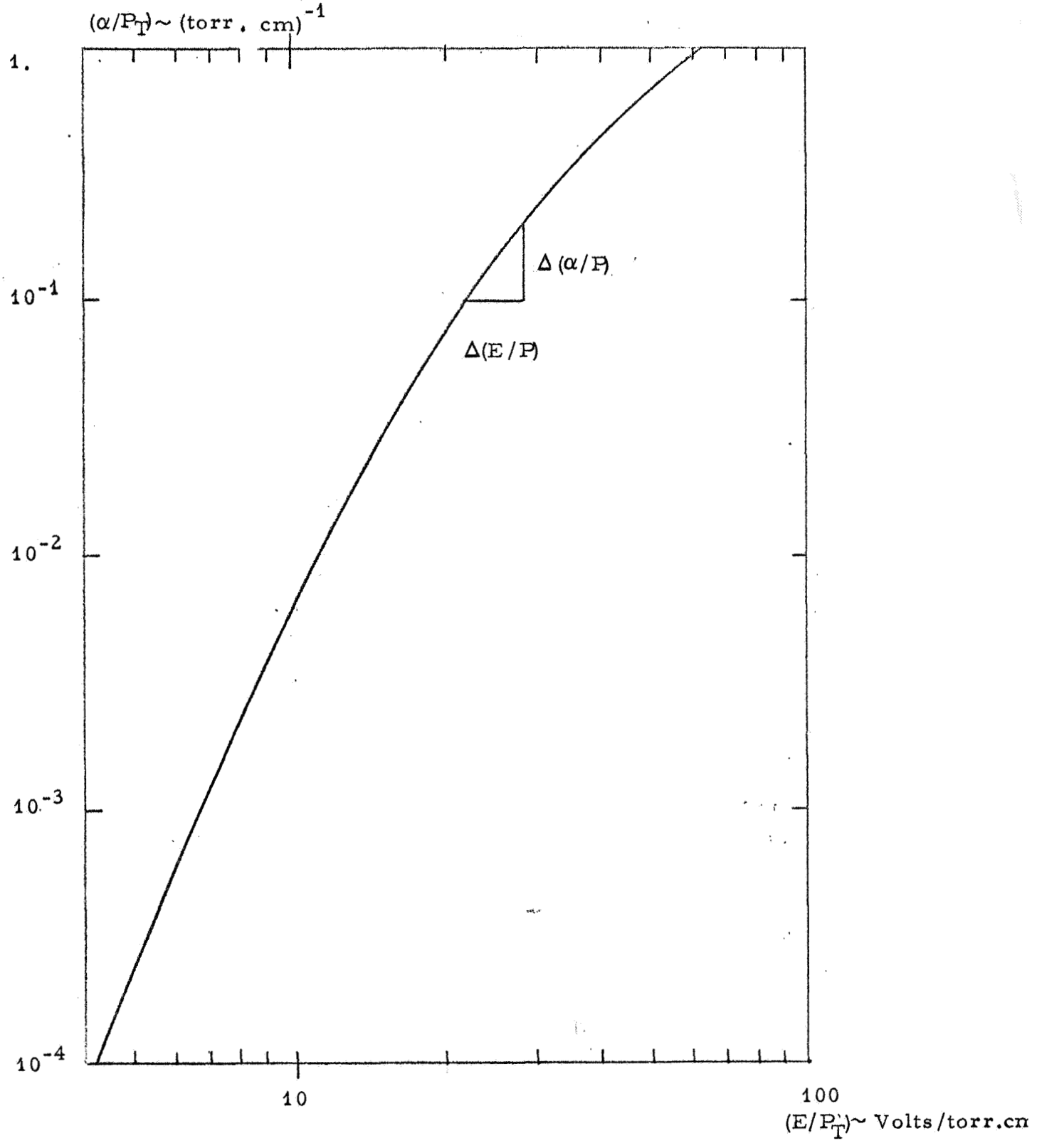

IONIZATION COEFFICIENT FOR
PURE ARGON (REF. 11)

FIGURE 8

FRANKLIN GNO CORPORATION

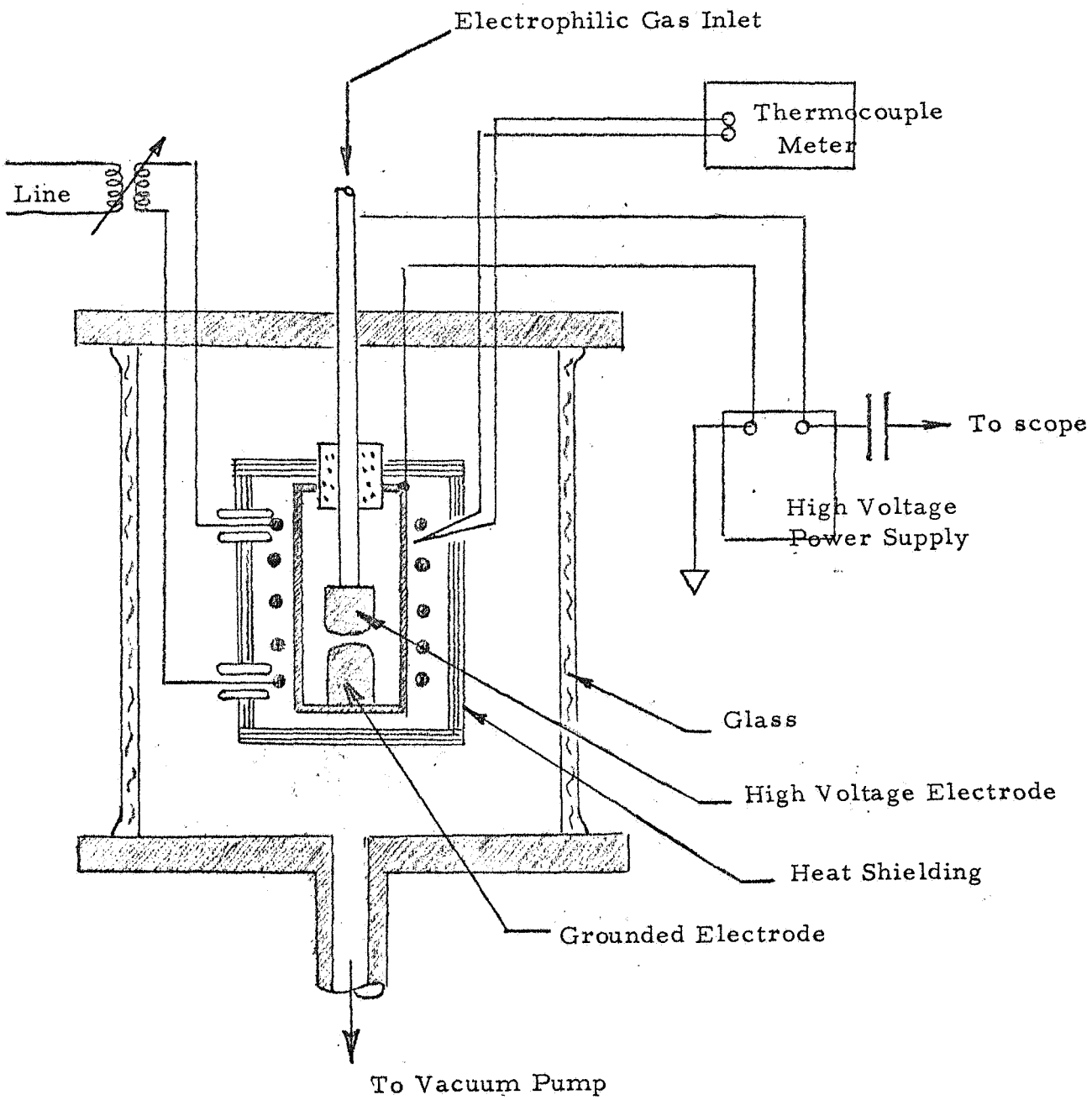

1000°C STATIC GAS BREAKDOWN

CELL SCHEMATIC

FIGURE 9

FRANKLIN GNO CORPORATION

To calibrate at higher temperatures, two effects are important:

- Thermal expansion of the electrodes, which tends to decrease the gap in this apparatus
- Reduced gas density in the gap which can be taken into account by

$$V_s = k_1 \; P\delta \; (T_o/T) \; + k_2. \tag{4-4}$$

Pure SF_6 heated up to 400°C was used to establish that these corrections were sufficient to account for the observed decrease in breakdown with temperature in the absence of chemical decomposition.

To check the gas mixture method, SF_6 and argon were measured together. Room temperature breakdowns occurred at $E/P_T = 430/(.157 \times 254)$ = 10.8 volts/torr . cm, where the argon and SF_6 vapor pressures were 254 and 1.3 torr respectively. For argon alone at 254 torr, the measured breakdown in the same apparatus occurred at $E/P_T = 8.8$, for which α/P_T argon = 3.5×10^{-3} $torr^{-1}$. cm^{-1} (ref. 12). For SF_6 & argon $\alpha/P = 8.2 \times 10^{-3}$, therefore the change in α/P_T caused by SF_6, but measured along the argon characteristic, is $\Delta(\alpha/P_T) = 4.7 \times 10^{-3}$. That is, $\Delta\alpha = \Delta\eta = (4.7 \times 10^{-3})(254) = 1.19$ cm^{-1}, and $\eta/P = 1.19/1.3 = 0.92$.

The measured value of 0.92 for SF_6 compares favorably with that of about 1.2 given in Ref. 11 (Figure 7), so that meaningful comparison of the present data, particularly at high temperatures can be obtained.

The experimental breakdown data obtained for several test gases Freons E-9, E-5, E-3, FC-43, and C_8F_{18} are shown in Figures 10, and 11.

These breakdown data have been reduced to equivalent attachment data, and appear in Figure 12. Because gas density in the breakdown gap (and gap spacing itself) change with temperature, computation in the form of corrections are required to derive suitable values of P_T and E/P_T for determination of η/P. Figure 12 shows the reduced data.

Referring to Figure 12, C_8F_{18} appears relatively insensitive up to 1000°C at the experimental value $E/P_T \approx 10$.

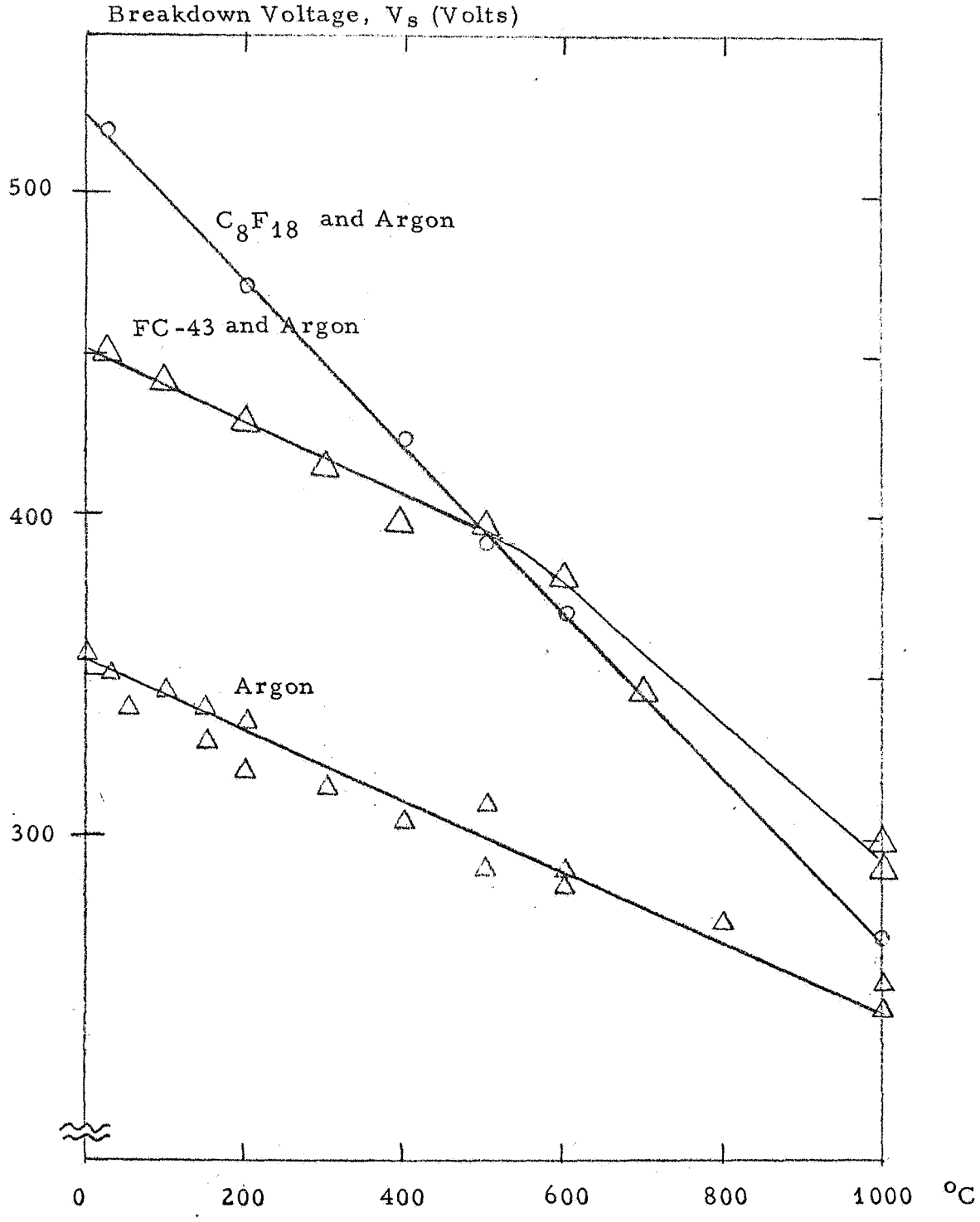

BREAKDOWN TO 1000°C FOR C_8F_{18} AND FC-43 AT DIFFERENT CONCENTRATIONS IN ARGON

FIGURE 10

FRANKLIN GND CORPORATION

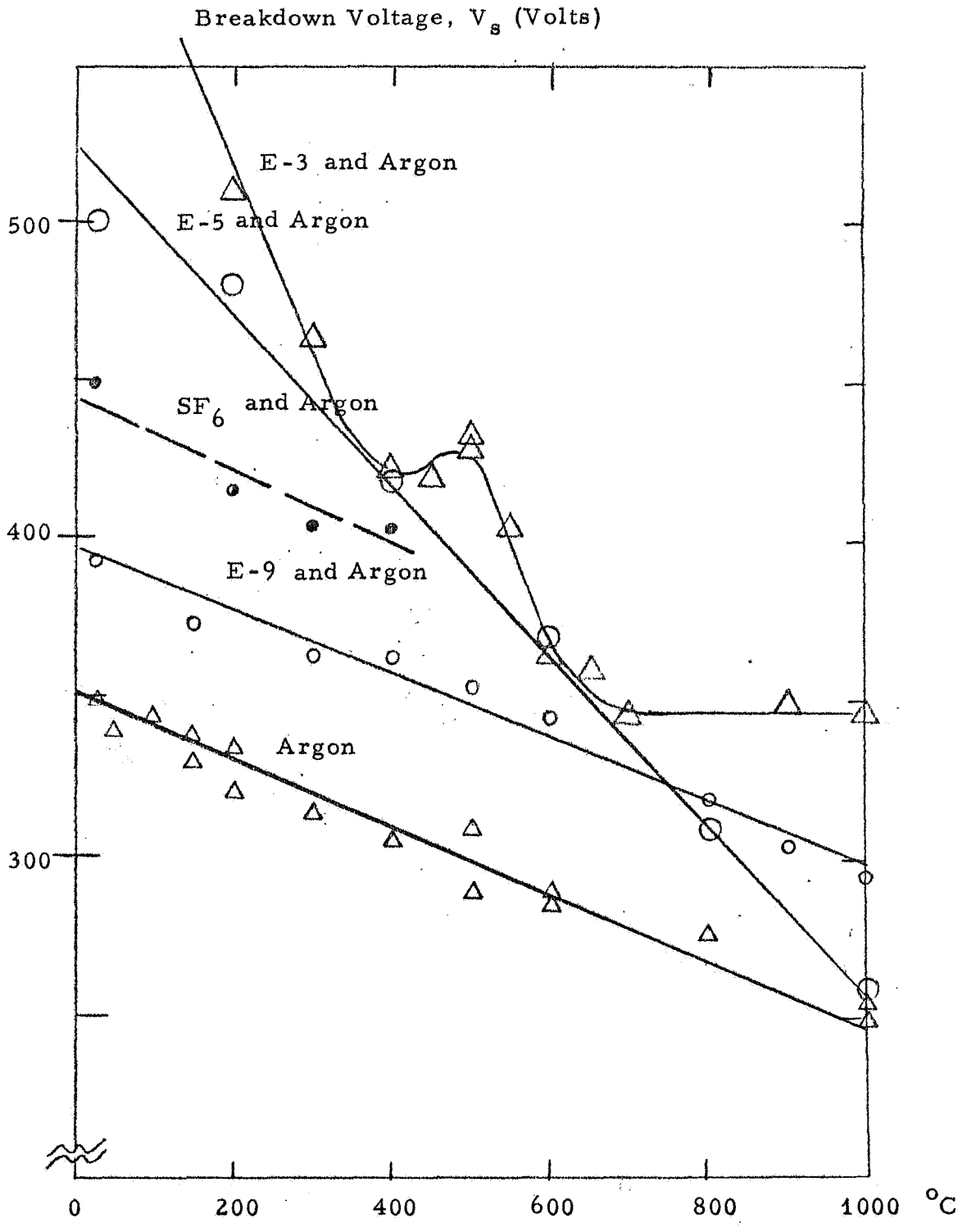

BREAKDOWN TO 1000°C FOR FREON E-9, FREON E-5, FREON E-3, AND SF_6 AT DIFFERENT CONCENTRATIONS IN ARGON

FIGURE 11

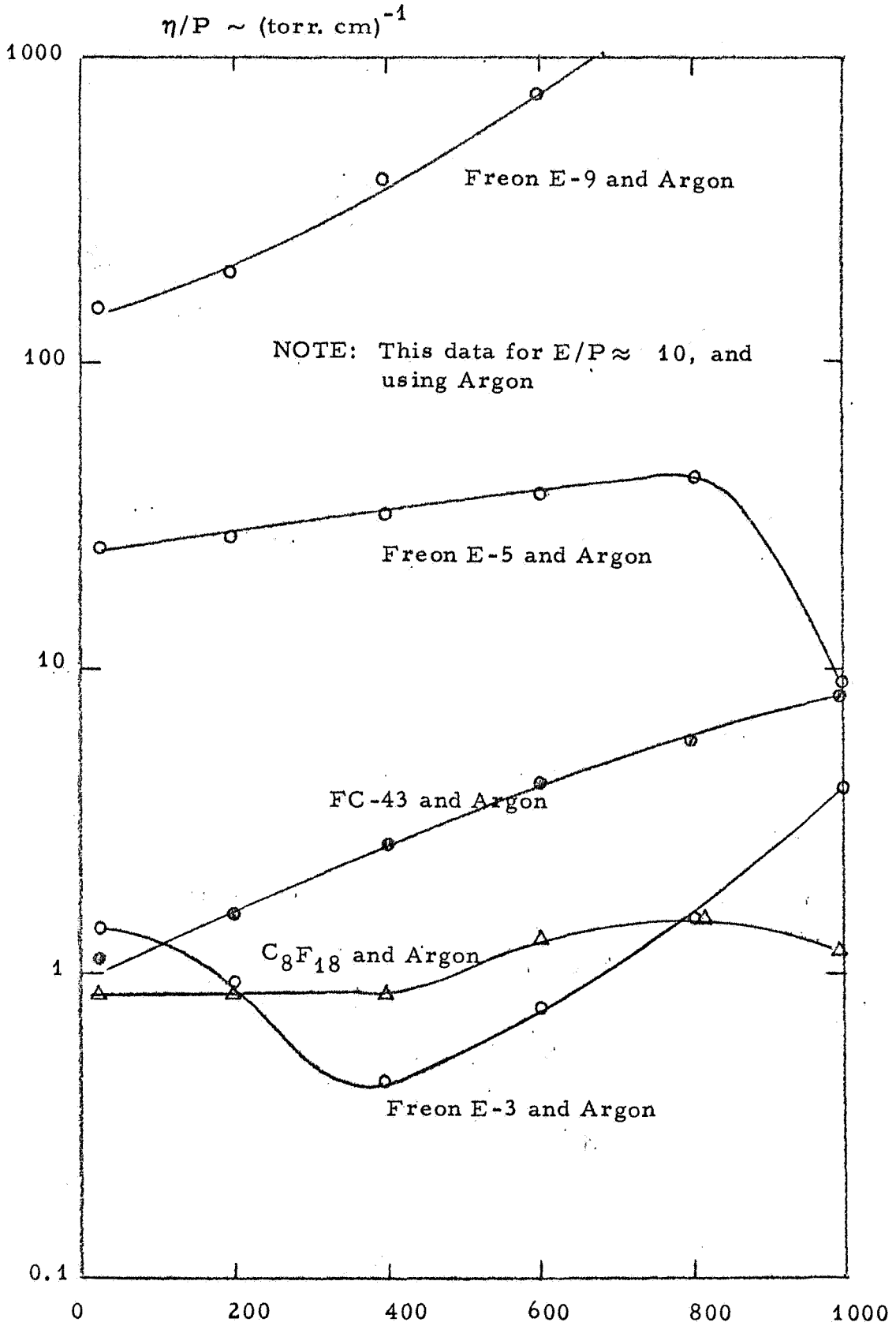

ATTACHMENT COEFFICIENT VS TEMPERATURE AT INTERMEDIATE VALUES OF E/P (Approximately 10), STATIC OVEN DATA

FRANKLIN GNO CORPORATION

FIGURE 12

FC-43 rises steadily in attachment as the temperature increases. Perhaps there are compound fragments formed which are also electrophilic so that the total of fragments may have higher attachment than the original compound. It is interesting to recall the presence of more than one negative ion species for C_7F_{16} described in Section 3-2-2. However, no fragment measurements were made for FC-43 or at high temperatures.

Of the Freon series, there is no regular behavior pattern. Attachment for E-3 at 1000°C, is increasing for E-5 is decreasing at the same temperature, and for E-9 is huge and undiminished by high temperature.

Conditions for each of the experimental curves in Figures 10 and 11 are included in Table V.

Calculated values of η/P for the above data are also included in Table V. Agreement between the values of η/P (at corresponding values of E/P_T) for the drift cell and the oven breakdown method at room temperature is excellent for E-3 and E-5 as well as for SF_6.

TABLE V

CONDITIONS FOR 1000°C OVEN BREAKDOWN AND VALUES OF η/P AT ROOM TEMPERATURE USING THE GAS MIXTURE METHOD

Materials	V_s (volts)	P (torr)	E/P_T	$\Delta(\alpha/P_T)$ (Ref. 11)	η/P (Room Temp)
Freon E-9	395	0.004	9.9	.0020	127.
Freon E-5	520	0.14	13.0	.0135	24.5
Freon E-3	650	6.5	16.3	.0345	1.35
SF_6	430	1.3	10.8	.0047	0.92
FC-43	450	1.4	11.3	.0045	0.82
C_8F_{18}	515	4.1	12.9	.0130	0.80
Argon	350	254	8.8	--	--

NOTES:

V_s = Breakdown voltage

P = Partial pressure of electrophilic additive

P_T = Total pressure of 254 torr for all above cases

δ = 0.157 cm at room temperature

$\alpha/P)$ argon = .0035 for $E/P)$ argon = 8.8

$\eta/P = (\overline{\Delta\alpha/P_T})\ (P_T/P)$

SECTION V

MOLECULAR BEAM BREAKDOWN UP TO 2000°C

Measurement of electron attachment in thermal equilibrium with hot surfaces is limited because of the background contributions from thermionic emission from the surfaces.

For the molecular beam experiments described in the following, the underlying principle is that cool electrodes may be used for the high temperature breakdown measurements if the hot gas is a flowing stream between the electrodes. The physical temperature of the electrodes is reduced by heat conduction through the electrodes so that the rate of energy received from the gas stream results in low electrode temperatures. Whereas gas jet expansion is used to form the molecular beam, there is relatively little effect on the mechanism for electrical breakdown because the mobility of the initiating electrons is high relative to the gas stream velocity. But this is not generally true for ions.

5-1 Background for Molecular Beam Experiments

Figure 13 shows the construction features of the high temperature beam apparatus used for the breakdown measurements. The vacuum environment and electrical hook-up is identical to that for the static oven breakdown tests.

Argon gas, after being bubbled through the liquid sample, was admitted through the gas inlet channel to the heat-exchange oven. A small exhaust orifice in the oven directed a stream of the argon and sample mixture to the test area between the electrodes.

Oven temperatures of 2000°C were measured with a tungsten 3%-rhenium versus tungsten 25%-rhenium thermocouple inserted inside the heat shield sheath of approximately 50 layers of .001" molybdenum sheet. The heater wire was tungsten, held loosely in place by a boron nitride bushing isolated from the path of the molecular beam.

The breakdown electrodes were 3/32 inches diameter and spaced about 1/16 inches apart.

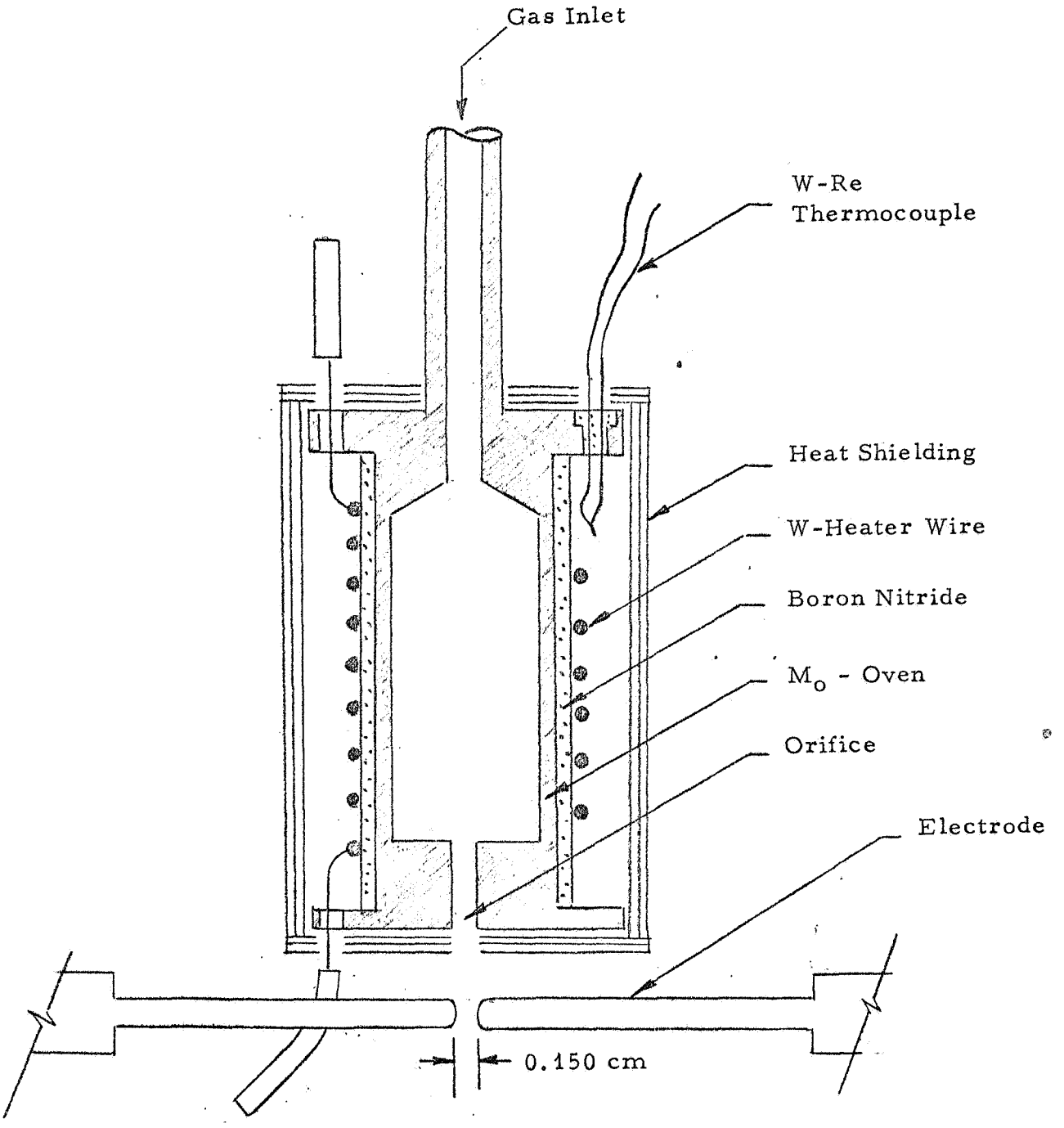

MOLECULAR BEAM HIGH TEMPERATURE
BREAKDOWN OVEN

FIGURE 13

Typical vacuum pressures in the vacuum chamber with flowing gas was about 30 torr while gas pressures in the test gap were 40 - 60 torr.

Pressures and partial pressures in the breakdown gap are a critical variable, and several calibration measurements were undertaken. The molecular beam profile was determined with a thermocouple moved across the beam cross section. The characteristic profile as determined about 1 mm downstream from the electrode, in a plane normal to the axes of the electrodes, is shown in Figure 14. The profile indicates departure of less than 10% in gas density from the average pressure in the gap.

In the procedure adopted for evaluation of the additives, only an approximate gas pressure in the gap is required. Under flow conditions argon breakdown voltage is first determined. Then, with flow reduced to zero, a static pressure is determined whereby an identical breakdown voltage occurs. Calibration of the gas flow in the gap in terms of equivalent static pressure for argon is shown in Figure 15. This method of pressure calibration by breakdown is compatible with results to be expected from the kinetics of gas flow through an orifice.

5-2 Molecular Beam Data

A typical experimental curve for molecular beam breakdown as a function of temperature is shown in Figure 16. Conditions for this and other materials tested are shown in Table VI.

Because these breakdown data are for a gas stream, calculations for η/P are more involved than for the static case, and also include greater errors. Values for η/P at room temperature obtained with the stream method are shown in Table VI for comparison with static oven data, and with other literature values. The agreement is satisfactory and permits a realistic evaluation of the high temperature attachment coefficients.

Figure 17 shows the reduced data for all high temperature runs in terms of η/P vs temperature. It is emphasized that the values of E/P_T are very high for these data (10 - 100 volts/torr . cm) so that the comparative influence of high temperature fragmentation is only partially examined for reentry applications. The attachment coefficient which is measured would be a natural sum of all fragment contributions.

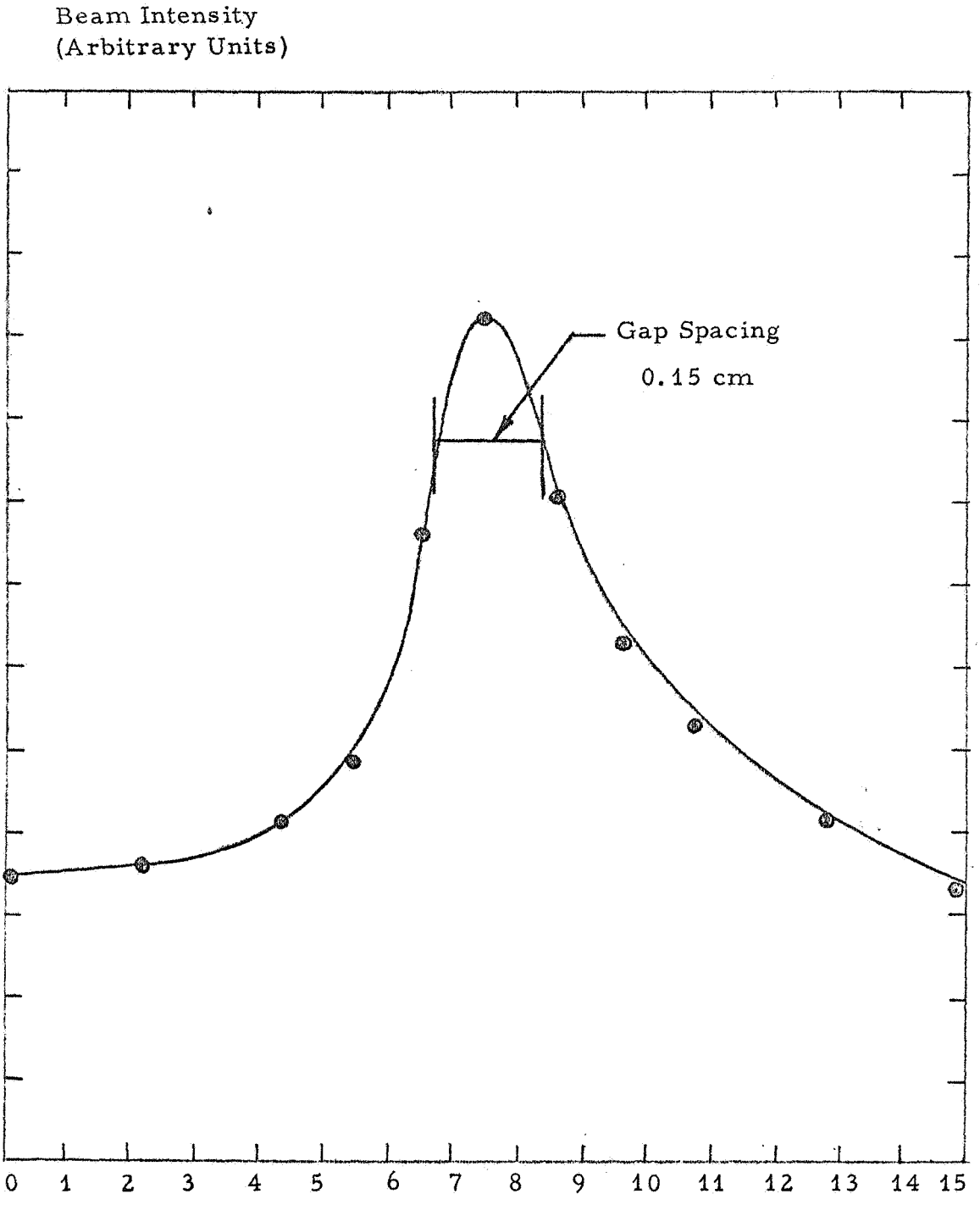

MOLECULAR BEAM PROFILE

FIGURE 14

FRANKLIN GNO CORPORATION

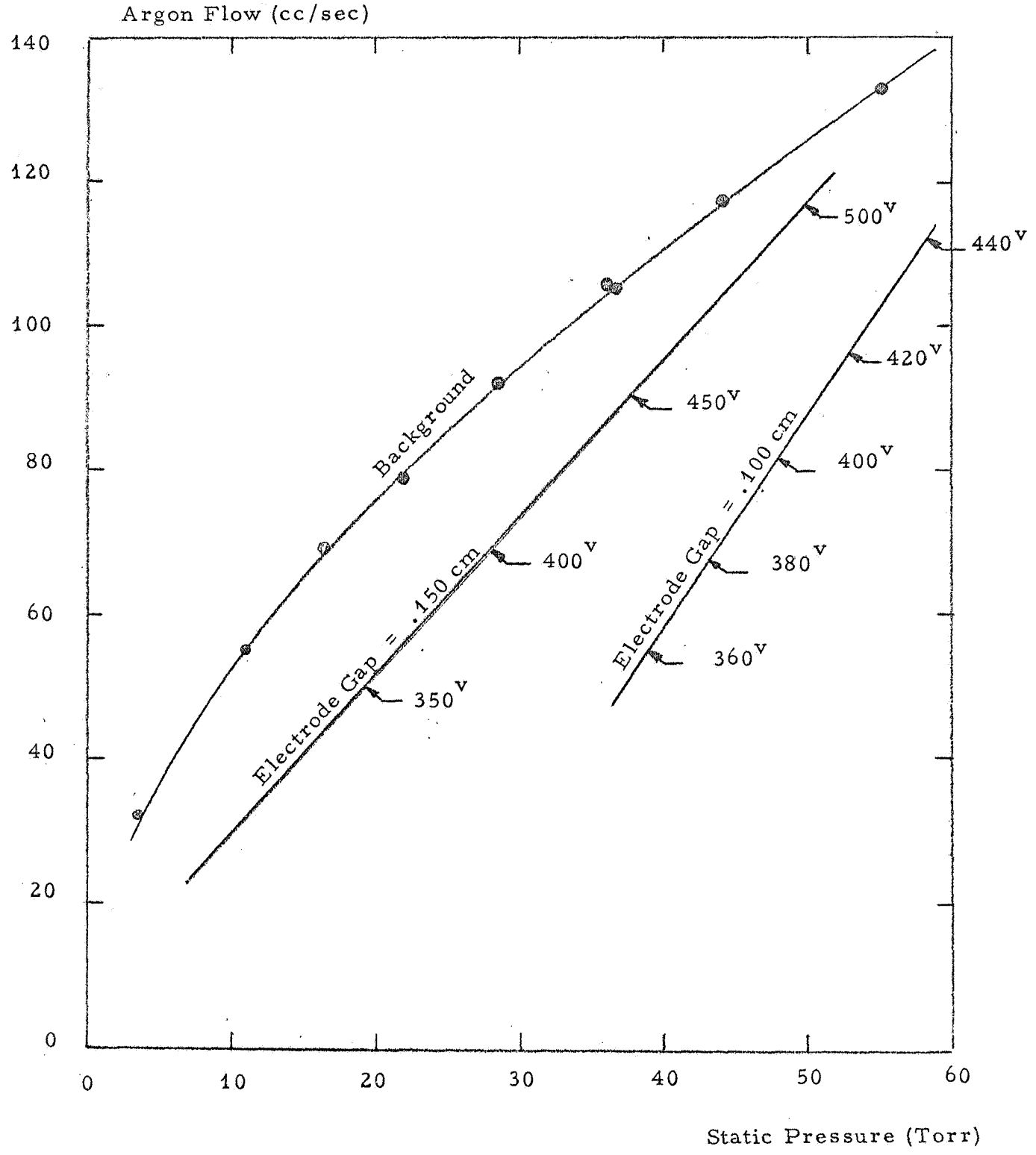

MOLECULAR BEAM PRESSURE CALIBRATION
FOR ARGON

FRANKLIN GNO CORPORATION

FIGURE 15

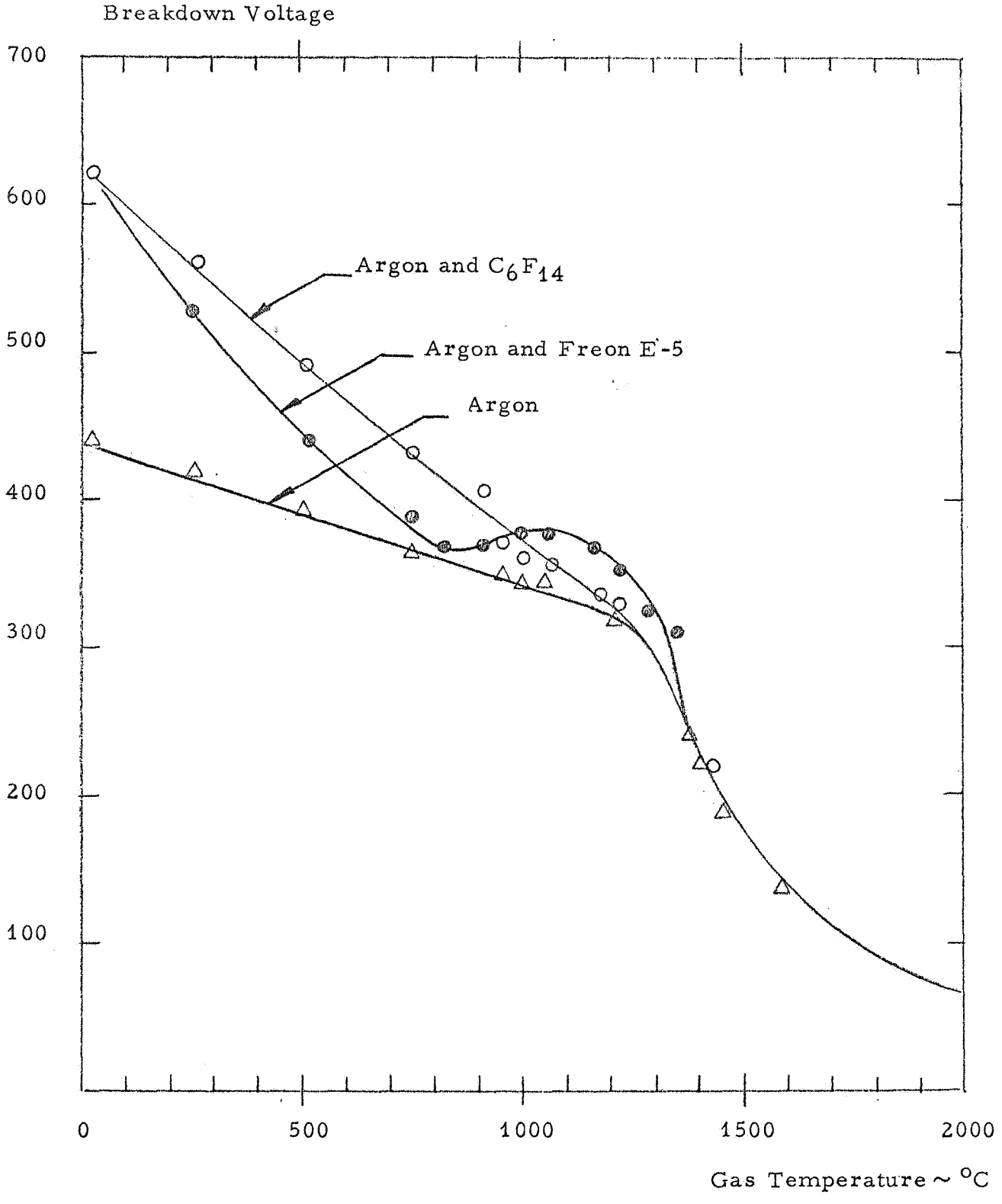

TYPICAL BREAKDOWN VOLTAGES OF MIXTURES
AS A FUNCTION OF TEMPERATURE

FIGURE 16

TABLE VI

DATA FOR 2000°C MOLECULAR BEAM BREAKDOWN

	P (torr)	$(P_T)_\delta$ (torr)	V_s (volts)	$E/(P_T)_\delta$	$\Delta\ \alpha/(P_T)_\delta$	η/P_δ	M (amu)
Freon E-9	.006	38	470	82.5	0.16	25.	1617
Freon E-5	1.5	38	530	93.	0.89	.95	949
Freon E-3	3.6	38	620	110	0.43	.28	617
FC-43	2.0	38	500	88.	0.30	.34	671
C_6F_{14}	20.	38	620	110	0.89	.20	338
C_8F_{18}	30.	51	540	106	0.74	.13	438
SF_6	22.6	38	570	100	0.61	1.02	146
Argon	--	38	435	76	--	--	40
Argon	--	51	370	72.5	--	--	40

NOTES:

- P is electrophilic pressure on the upstream side of the orifice.
- $(P_T)_\delta$ is the total pressure equivalent in the breakdown gap.
- All breakdown gap spacings are 0.150 cm except for C_8F_{18} data and argon at 51 Torr.

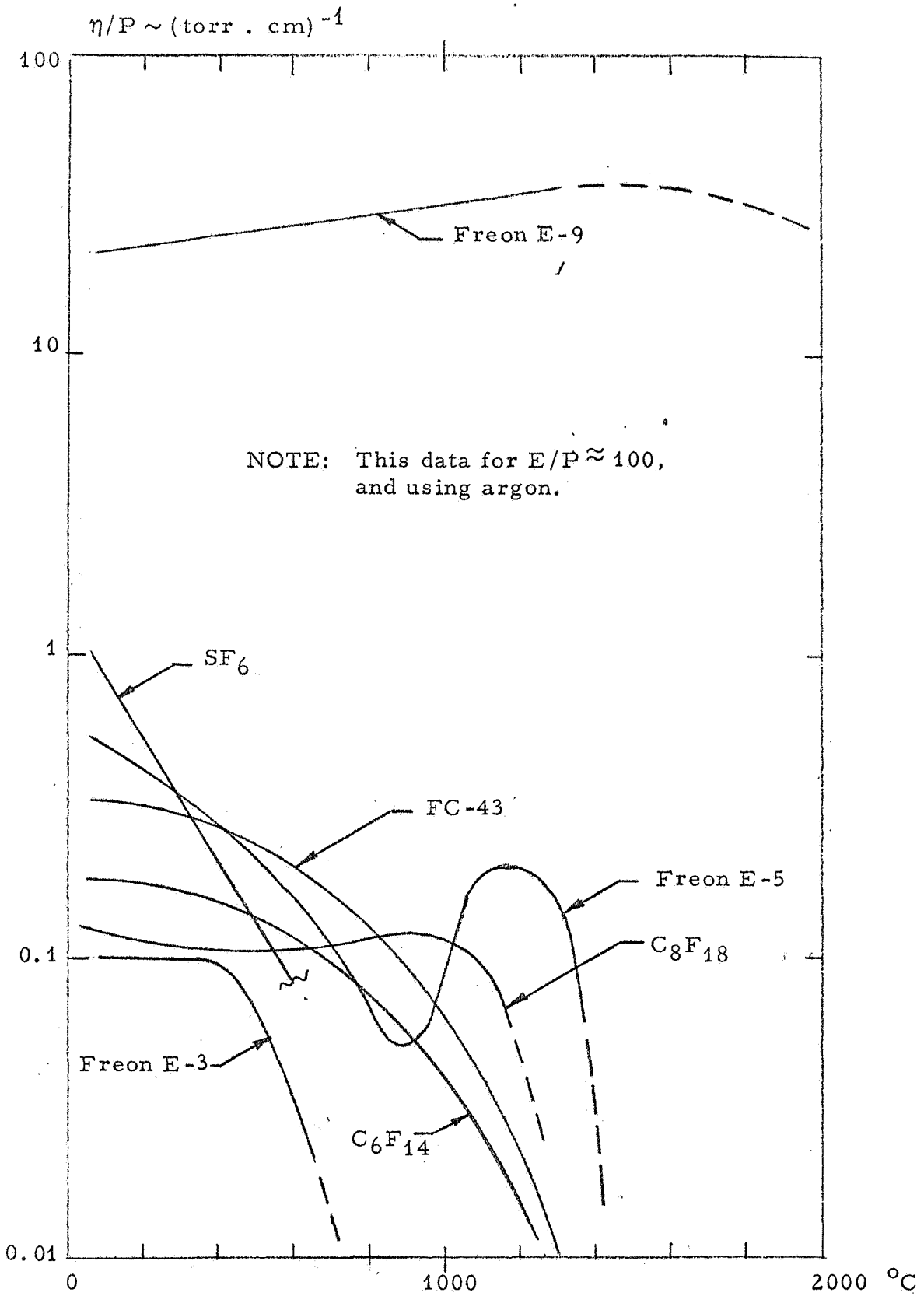

ATTACHMENT COEFFICIENT VS TEMPERATURE
AT HIGH VALUES OF E/P_T (Approximately 100)

FIGURE 17

The effective region for reentry blackout is $1 < E/P_T < 10$, even for the highest reentry temperatures. It appears possible that the experimental data obtained with the present beam method can be extended to lower values of E/P_T with modification of the technique.

SECTION VI

SUMMARY AND CONCLUSIONS

1. Electron attachments for several fluorocarbon materials were determined, and the results for room temperature gas are tabulated in Table VII. The significant value which gives a measure of the electron attachment as shown is η/P, where η is the attachment coefficient (number of attachments per cm), and P is the electrophilic gas pressure. The ratio η/P can be associated with the electron attachment cross-section, and the quantity E/P_T* is a measure of the average electron energy derived from the applied electric field. Therefore Table VII indicates that electron attachment varies with the energy of the electrons to be attached. Materials examined, in general order of decreasing attachment were: Freon E-9, Freon E-5, Freon E-3, C_8F_{18}, C_7F_{16}, C_6F_{14}, FC-43, and SF_6.

2. Electron attachment was found to generally decrease with increasing gas temperatures up to 2000°C, except for Freon E-9. In order of decreasing temperatures for the upper limit of attachment: Freon E-9, Freon E-5, C_8F_{18}, FC-43, C_8F_{14}, SF_6, and Freon E-3.

3. Detailed variation of electron attachment with gas temperatures can be found up to 2000°C in Figure 17 ($E/P_T \approx 10$), of the text.

4. Of all materials examined, Freon E-9 has the greatest value of η/P and remains essentially unchanged up to 2000°C. At room temperatures, and for $E/P_T \approx 10$ the attachment of Freon E-9 was about two orders greater than that for SF_6.

5. The reduced mobilities in nitrogen for Freon E-5, Freon E-3, C_7F_{16} (No. 1 peak), and C_7F_{16} (No. 2 peak) observed for room temperature gas were 0.56, 0.47, 0.34 and 0.70 respectively over a concentration range of 0 - 10%.

6. Two new methods were developed for the measurement of electron attachment of highly electrophilic gases. A method of mixtures was used, whereby changes in the electrical breakdown of argon due to the presence of trace gases could be interpreted for determination of η/P. In addition, a molecular beam was adapted to breakdown measurement so that high temperature electron attachment data could be obtained.

---

*P is electrophilic pressure, P_T is total gas pressure (see P 3-2)

TABLE VII

SUMMARY OF VALUES OF η/P^* AT ROOM TEMPERATURE

Materials	(amu)	Drift Cell (Nitrogen) $E/P_T = 1$	Static Breakdown (Argon) $E/P_T \approx 10$	Beam Breakdown (Argon) $E/P_T \approx 100$
Freon E-9	(1617)	--	127	25
Freon E-5	(949)	30	24.5	0.46
FC-43	(671)	--	0.82	0.34
Freon E-3	(617)	2	1.35	0.61
C_8F_{18}	(438)	--	0.80	0.13
C_7F_{16}	(388)	6.5	--	
C_6F_{14}	(338)	--	--	0.20
SF_6	(146)	--	0.92	1.02
O_2	(32)	0.03	--	--
$O_2 \rightarrow O$	(16)	--	0.1	.03

NOTES:

- Drift cell values are an average (See Figure 7 in text)
- O and O_2 data are literature values (Reference 10)

*η/P is a measure of electron attachment cross-section (Ref. 3-2)

7. Although C_7F_{16} is not the most interesting candidate for reentry applications, it is the only material tested which was observed to occur as two species (see Figure 5 in the text). Reasons for the effect are obscure at the moment.

8. No total pressure effects have been observed for the electron attachment process which occurs at room temperature in the drift cell. Therefore it is presumed that the negative ion lifetimes are longer than collision times with background gases. This would be expected generally because the high attachment for larger molecules would have long lifetimes and lead readily to stable negative ion formation.

REFERENCES

1. "The Entry-Communications Problem", P. W. Huber and T. E. Sims, Astronautics and Aeronautics, p. 31 (Oct. 1964).

2. "Injection and Distribution of Liquids in the Flow of Fields of Blunt Shapes at Hypersonic Speeds", NASA TM X-989 (1964), Confidential

3. "RAM-B2 Flight Test of a Method for Reducing Radio Attenuation During Hypersonic Reentry," NASA TM X-902 (1963).

4. Charge Recombination on Water Droplets in a Plasma", NASA TM X-1186, J. S.. Evans.

5. "Reentry Plasma Studies", T. E. Sims and W. L. Grantham, Proceedings Conference Application of Plasma Studies to Reentry Vehicle Communication, Vol. I, Dayton, Ohio, October 3-4, 1967.

6. "Fluorocarbons and Their Derivatives", R. E. Banks, Oldbourne Press, London (1964).

7. "Fluorine Chemistry", J. H. Simons, Academic Press, N. Y. (1950).

8. "A Fundamental Study of Electrophilic Gases for Plasma Quenching", R. W. Crowe and W. D. Kilpatrick, NASA CR-66206, (1966).

9. "Boxcar Integrator, Model CW-1", Princeton Applied Research Corporation, Princeton, N. J.

10. "Measurements of the Attachment of Low-Energy Electrons to Oxygen Molecules", L. M. Chanin, A. V. Phelps, and M. A. Biondi, Phys. Rev. 128, p. 219 - 230, (1962).

11. R. Geballe and M. L. Reeves, Phys. Rev. 92, 867 (1953).

12. A. A. Kruithoff, Physica 7 519 (1940), (Ref. Basic Processes of Gaseous Electronics, L. B. Loeb, p. 692 (1955)).

DISTRIBUTION LIST

NASA Langley Research Center
Langley Station
Hampton, Virginia 23365
Attention: Norman D. Akey,
Mail Stop 473

NASA Langley Research Center
Langley Station
Hampton, Virginia 23365
Attention: R. L. Zavasky,
Mail Stop 117

NASA Ames Research Center
Moffett Field, California 94035

NASA Flight Research Center
P. O. Box 273
Edwards, California 93523

Jet Propulsion Laboratory
4800 Oak Grove Drive
Pasadena, California 91103

NASA Manned Spacecraft Center
2101 Webster Seabrook Road
Houston, Texas 77058

NASA Marshall Space Flight Center
Huntsville, Alabama 35812

NASA Wallops Station
Wallops Island, Virginia 23337

NASA Electronics Research Center
575 Technology Square
Cambridge, Massachusetts 02139

NASA Lewis Research Center
21000 Brookpark Road
Cleveland, Ohio 44135

NASA
Washington, D. C. 20546

NASA Goddard Space Flight Center
Greenbelt, Maryland 20771

NASA Michoud Assembly Facility
P. O. Box 26078
New Orleans, Louisiana 70126

NASA John F. Kennedy Space Center
Kennedy Space Center, Florida 32899

AeroChem Research Laboratories, Inc.
P. O. Box 12
Princeton, New Jersey 08540
Attention: Dr. S. C. Kurzius

Aerotherm Corporation
460 California Avenue
Palo Alto, California 94306

Air Force Avionics Laboratory
Wright-Patterson Air Force Base,
Ohio 45433
Attention: Robert A. Simons

The Ohio State University Research
Foundation
ElectroScience Laboratory
1320 Kinnear Road
Columbus, Ohio 43212
Attention: Ross Caldecott

Air Force Cambridge Research
Laboratories
Electronic Research Directorate
L. G. Hanscom Field
Bedford, Massachusetts 01730
Attention: CRDM/Mr. Walter Rotman

NASA Scientific and Technical
Information Facility
P. O. Box 33
College Park, Maryland 20740